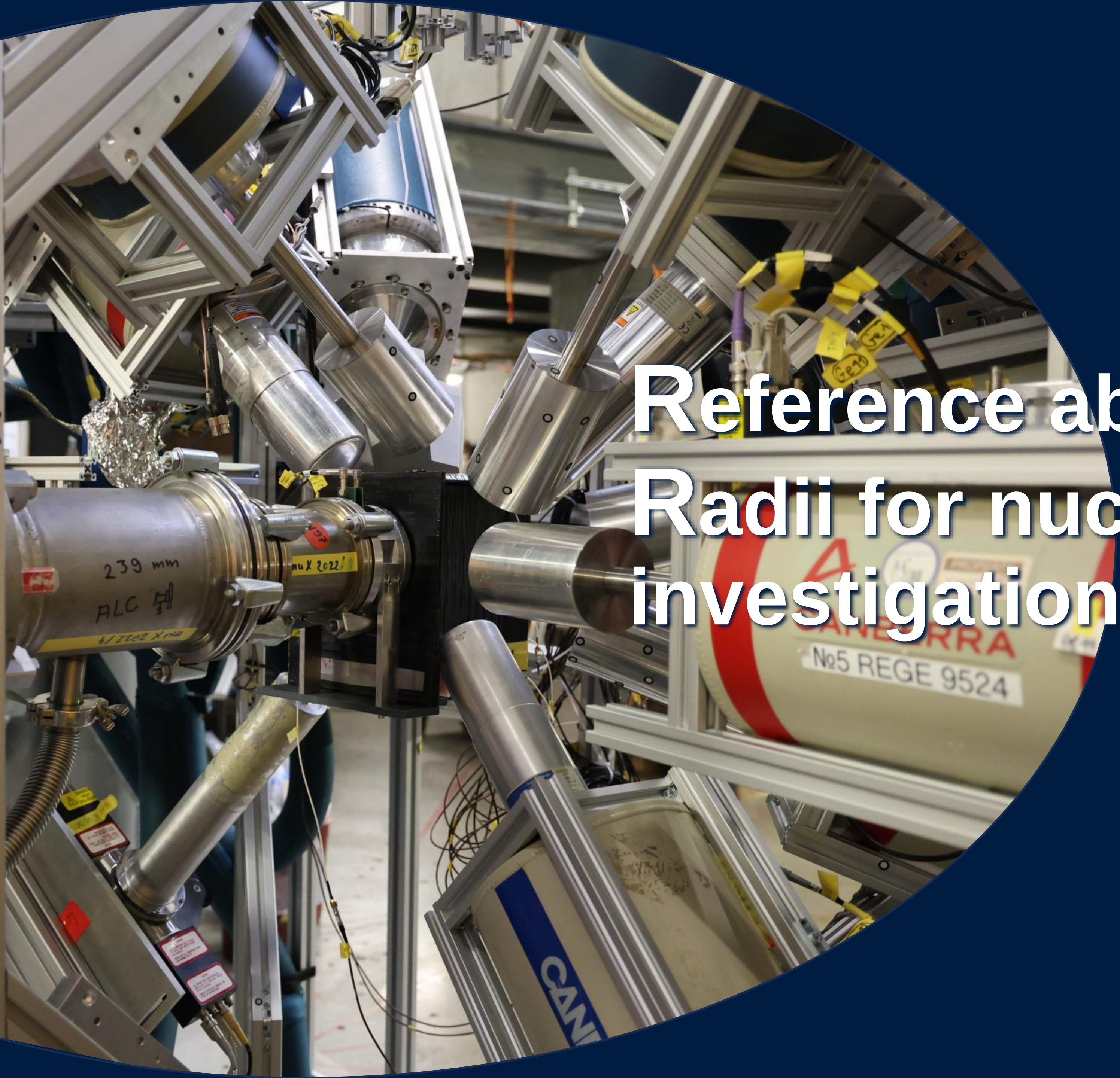

Reference absolute charge Radii for nuclear structure investigations of exotic nuclei

Reference Radii: Absolute radii across the nuclear landscape

Nuclear radii for nuclear structure

- How do nuclei and nuclear matter emerge from the underlying fundamental interactions?
- What shapes can nuclei take, how do nuclear shells evolve, and what role do nuclear correlations play?
- What are the limits of the existence of nuclei, and what phenomena arise from open quantum systems?

- Nuclear charge radii reveal changes in nuclear shapes across the nuclear landscape.
  - From spherical nuclei near closed shells to prolate and oblate deformations.
- And to revealing exotic forms of matter like octupole deformed nuclei or investigating proton-unbound nuclei.

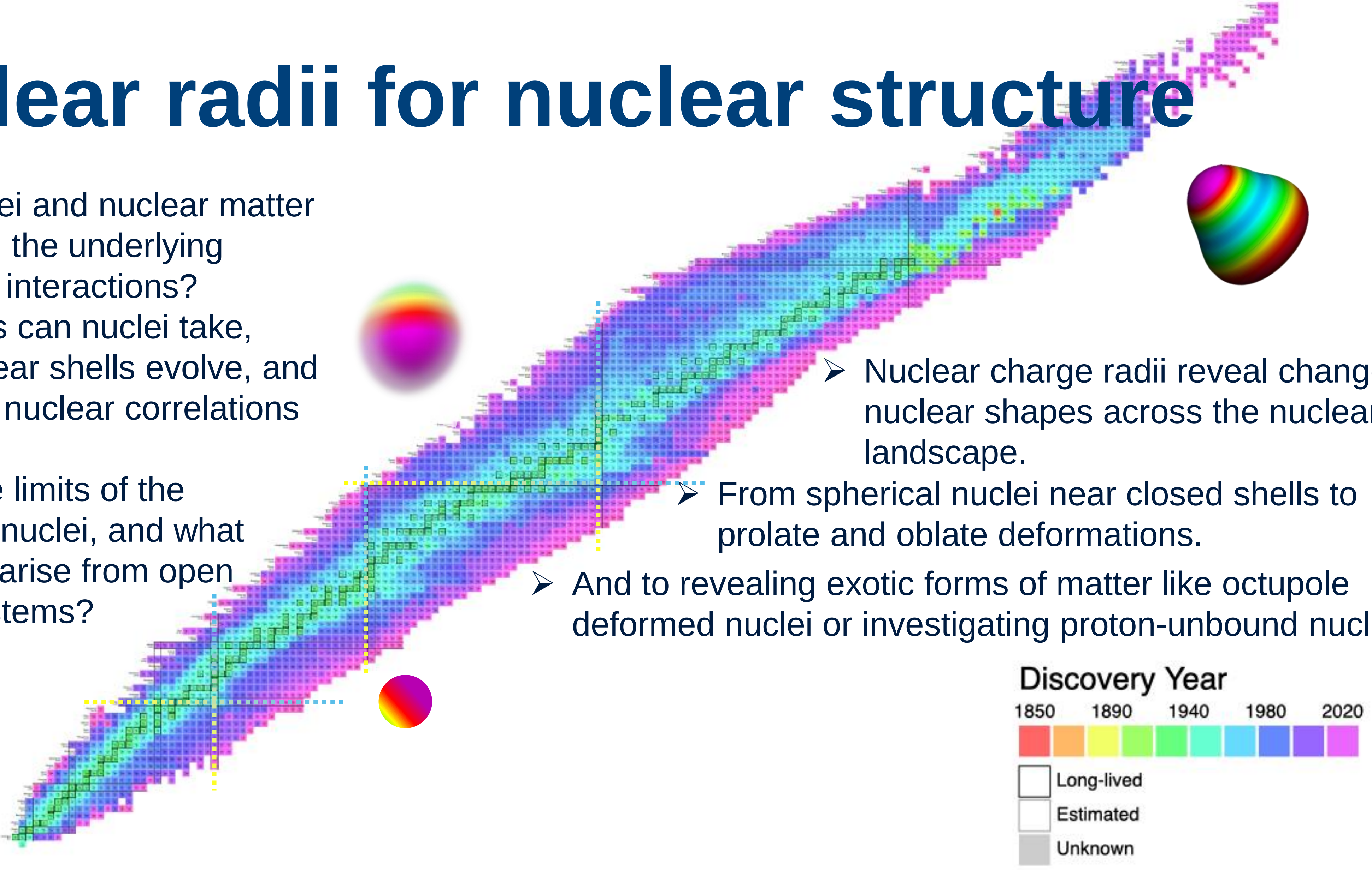

NuPECC Long Range Plan 2024, https://nupecc.org/lrp2024/Documents/nupecc_lrp2024.pdf
The Colourful Nuclear Chart, https://people.physics.anu.edu.au/~ecs103/chart/

Nuclear radii for fundamental interactions

E.g., V_{ud}

- The unitarity of the CKM matrix connecting the quark generations is a good test of the Standard Model.
- V_{ud} is largest first-row element. That row provides the most stringent limit on this unitarity and V_{ud} dominates the uncertainty. It is mainly determined by superallowed $0^+ \rightarrow 0^+$ Fermi β decays.
- The nuclear charge radius affects the statistical rate function (f) and isospin-symmetry breaking correction (δC) that are part of the determination of V_{ud}.

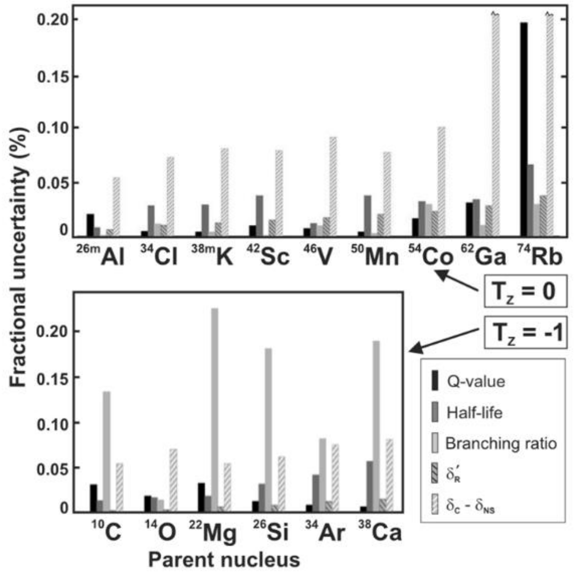

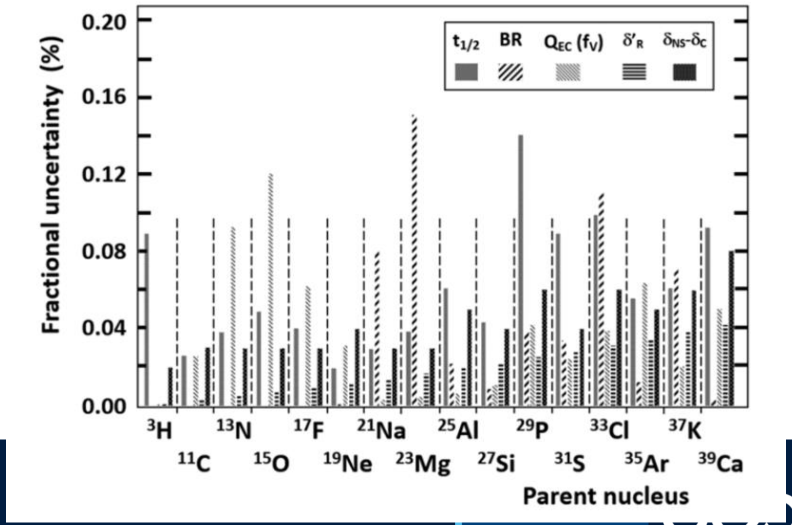

*J. Hardy & I. Towner. PRC **102** (2020) 045501.*
*N. Severijns, L. Hayen et al. PRC **107** (2023) 015502.*

Probing the nucleus through its electrons

Use lasers to scan for transition energies

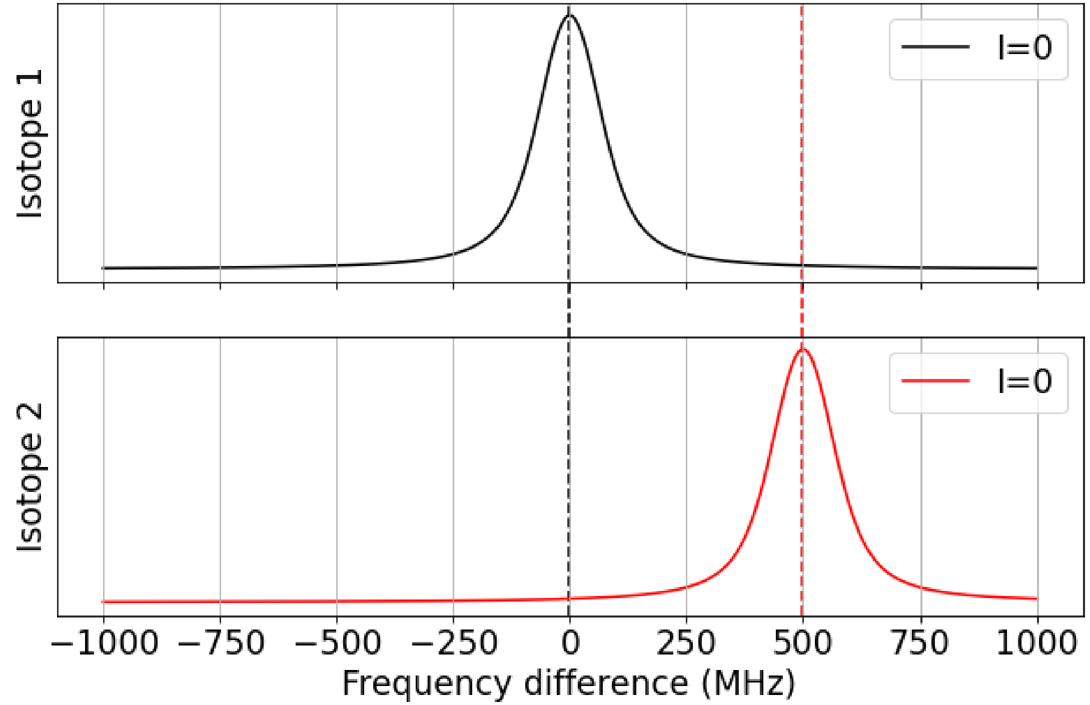

Extract isotope shifts $\delta\nu^{A,A'}$ → Infer $\delta < r^2 >^{A,A'}$

$$\delta < r^2 >^{A,A'} = \frac{1}{F}\left(\delta\nu^{A,A'} - M\,\frac{m_{A'} - m_A}{m_A\, m_{A'}}\right)$$

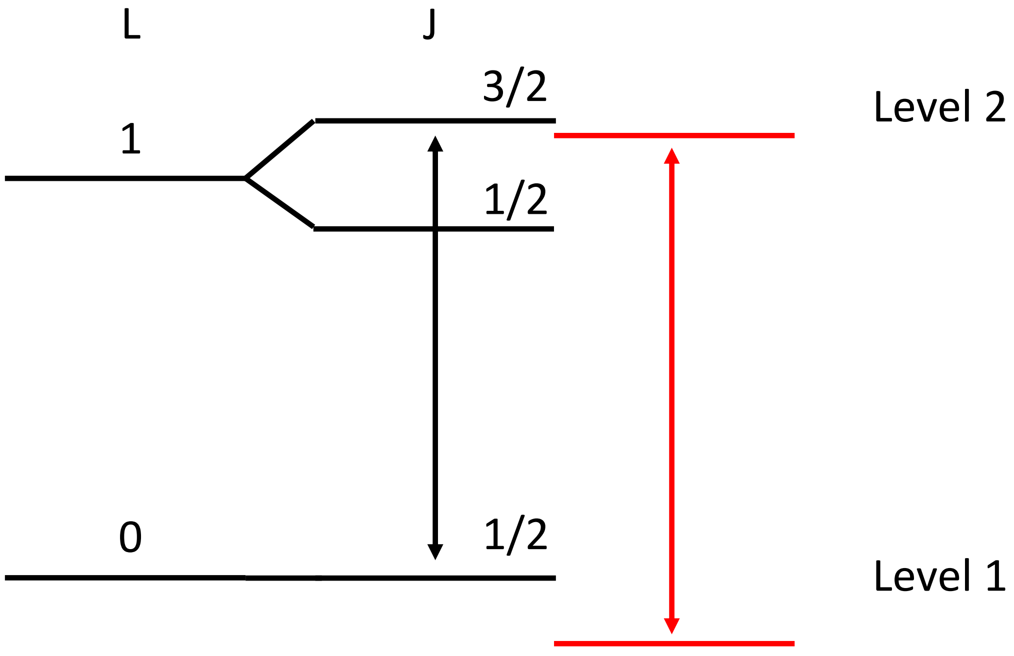

I = 0 → No hyperfine splitting

King plot against absolute radii

$$\delta\langle r^2\rangle^{A,A'} = \frac{1}{F_i}\left(\delta\nu_i^{A,A'} - \frac{A - A'}{A\,A'} M_i\right)$$

- M_i : Mass shift factor
- F_i : Field shift factor

$$\frac{A\,A'}{A - A'}\,\delta\nu_i^{A,A'} = M_i + F_i\,\frac{A\,A'}{A - A'}\,\delta\langle r^2\rangle^{A,A'}$$

No odd-Z element with 3 stable isotopes!

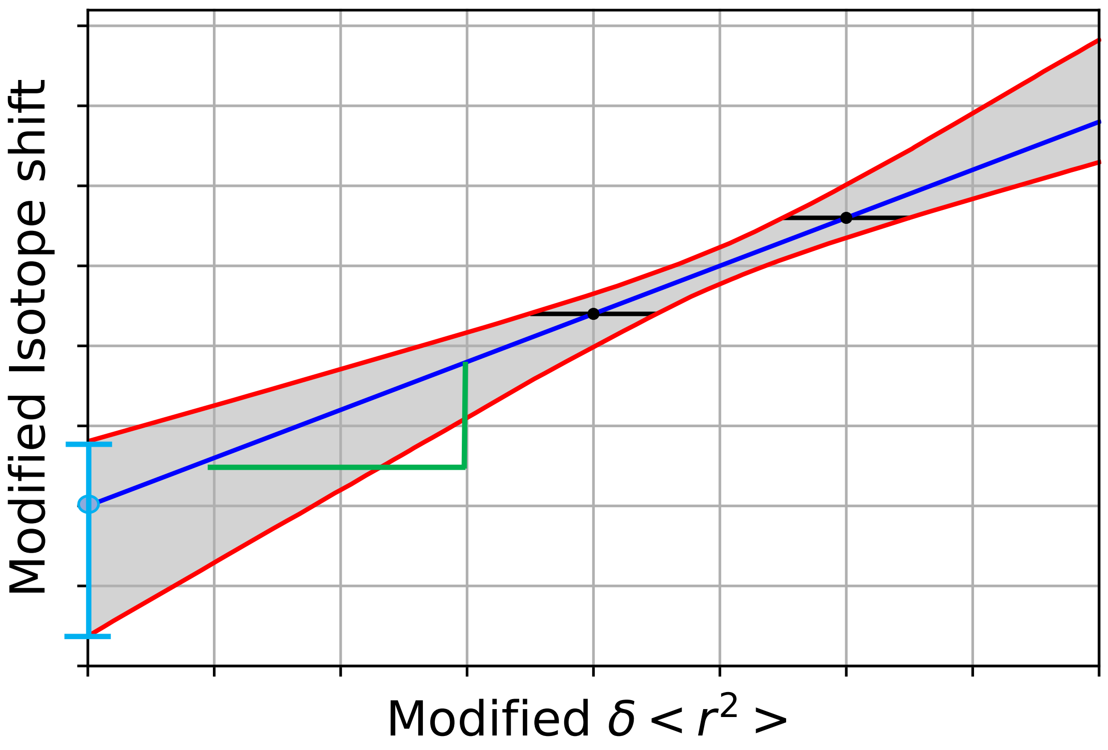

Experimental technique: Muonic x-ray spectroscopy

μ-atomic spectroscopy with GIANT at PSI

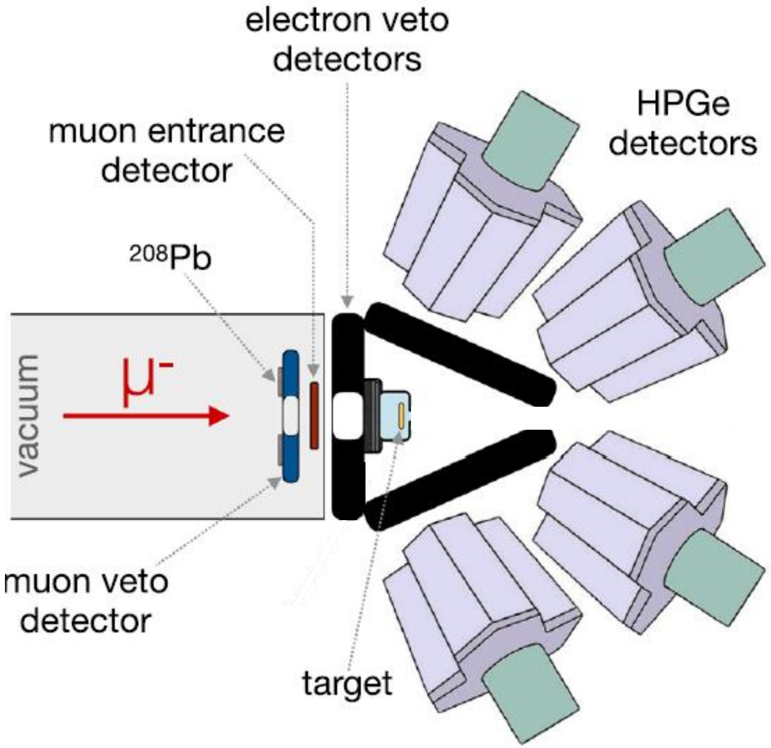

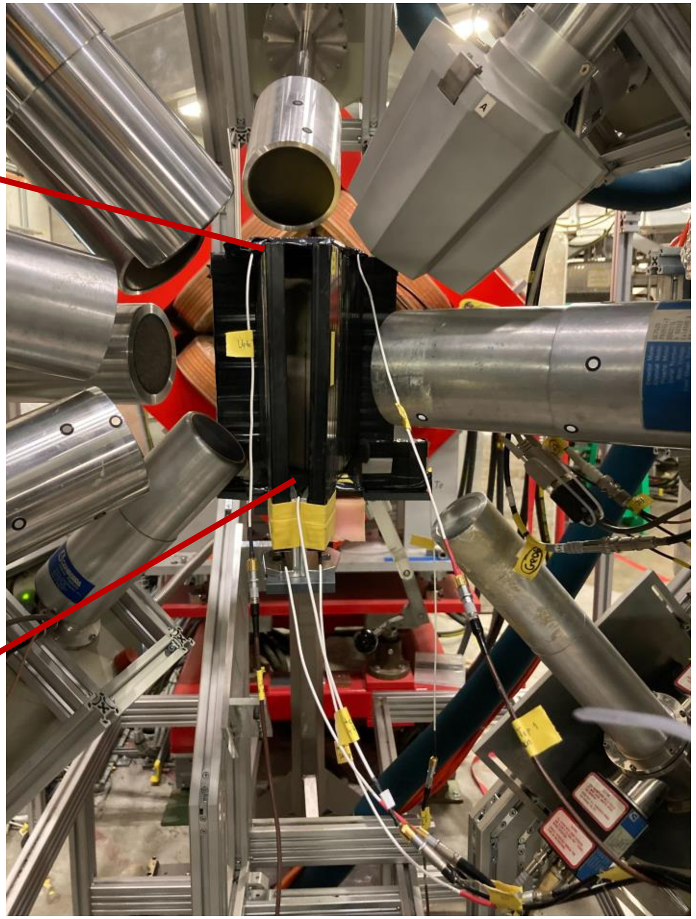

Synergies with the MIXE collaboration

A. Adamczak et al., *Muonic atom spectroscopy with microgram target material, Eur. Phys. A* ***59*** *(2023) 15.*
I. Gerchow et al., Germanium array for non-destructive testing (GIANT) setup for muon-induced x-ray emission (MIXE) at the Paul Scherrer Institute, Review of Scientific Instruments ***94*** *(2023) 045106.*

Measuring microgram materials

Traditionally: Limited to target mass O(10-100 mg)

Hydrogen gas cell (100 bars; 0.25% deuterium)

- Limited to O(5 µg)
- Down to 20 year half-life (radioprotection)

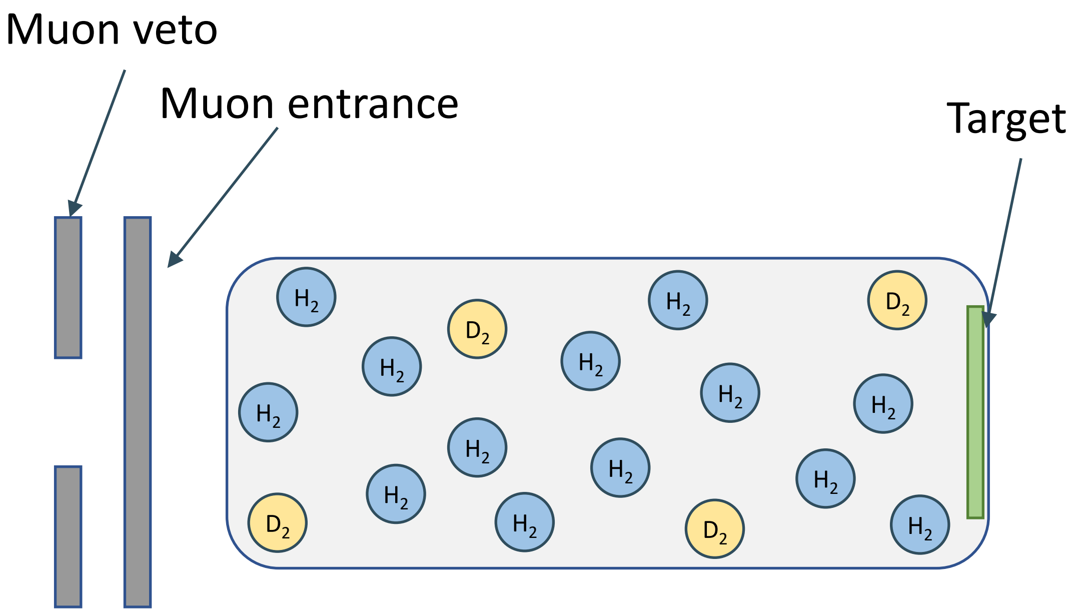

Bubak, M., & Fajman, M. P. (1987). Cross sections for hydrogen muonic atomic processes in two-level approximation of the adiabatic framework (No. JINR-E--4-87-464). Joint Inst. for Nuclear Research.
*Adamczak, Andrzej, et al. "Muonic atom spectroscopy with microgram target material." The European Physical Journal A **59** (2023): 15.*

KU LEUVEN

Measuring microgram materials

Traditionally: Limited to target mass O(10-100 mg)

Hydrogen gas cell (100 bars; 0.25% deuterium)

- Limited to O(5 µg)
- Down to 20 year half-life (radioprotection)

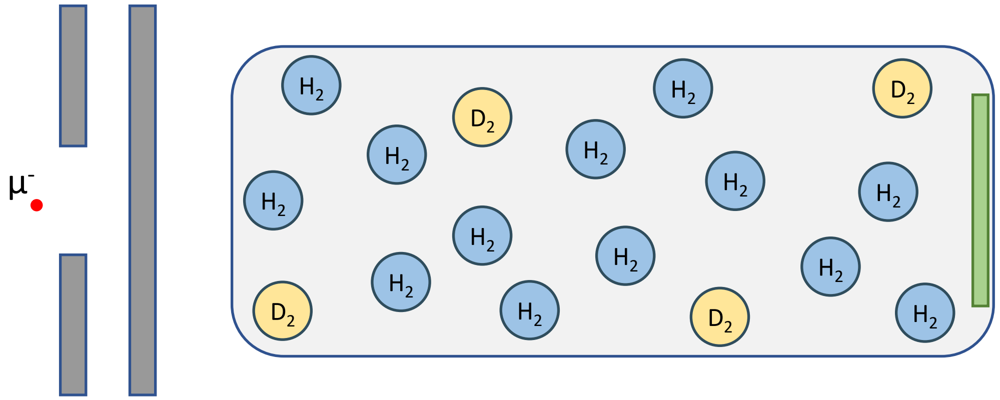

Bubak, M., & Fajman, M. P. (1987). Cross sections for hydrogen muonic atomic processes in two-level approximation of the adiabatic framework (No. JINR-E--4-87-464). Joint Inst. for Nuclear Research.
Adamczak, Andrzej, et al. "Muonic atom spectroscopy with microgram target material." The European Physical Journal A ***59*** *(2023): 15.*

KU LEUVEN

Measuring microgram materials

Traditionally: Limited to target mass O(10-100 mg)

Hydrogen gas cell (100 bars; 0.25% deuterium)

- Limited to O(5 µg)
- Down to 20 year half-life (radioprotection)

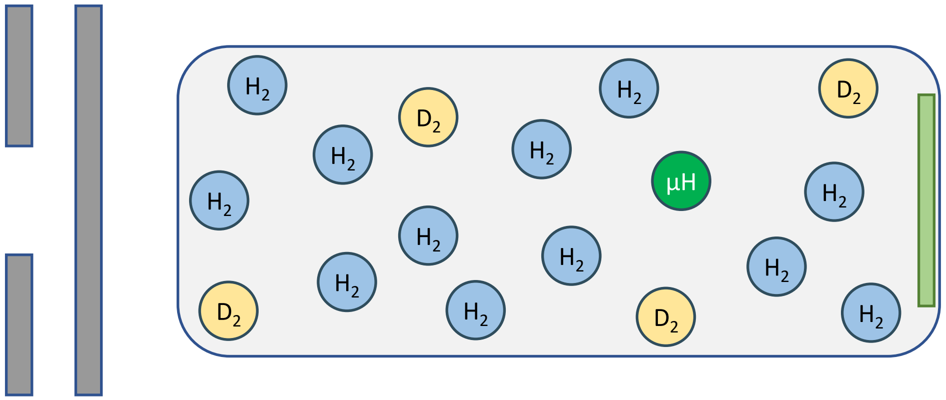

Bubak, M., & Fajman, M. P. (1987). Cross sections for hydrogen muonic atomic processes in two-level approximation of the adiabatic framework (No. JINR-E--4-87-464). Joint Inst. for Nuclear Research.

*Adamczak, Andrzej, et al. "Muonic atom spectroscopy with microgram target material." The European Physical Journal A **59** (2023): 15.*

Measuring microgram materi

Traditionally: Limited to target mass O(10-100 mg)

Hydrogen gas cell (100 bars; 0.25% deuterium)

- Limited to O(5 µg)
- Down to 20 year half-life (radioprotection)

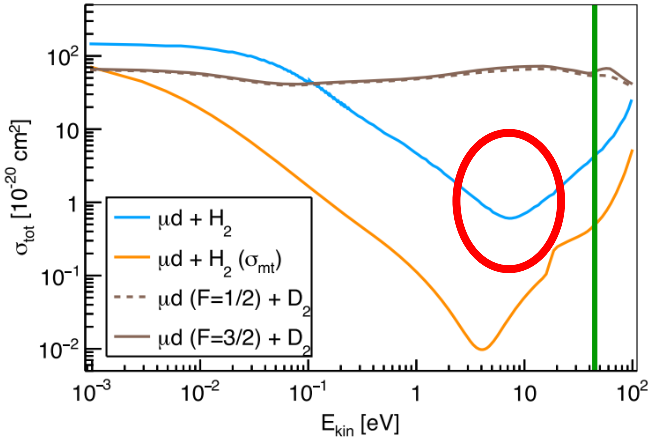

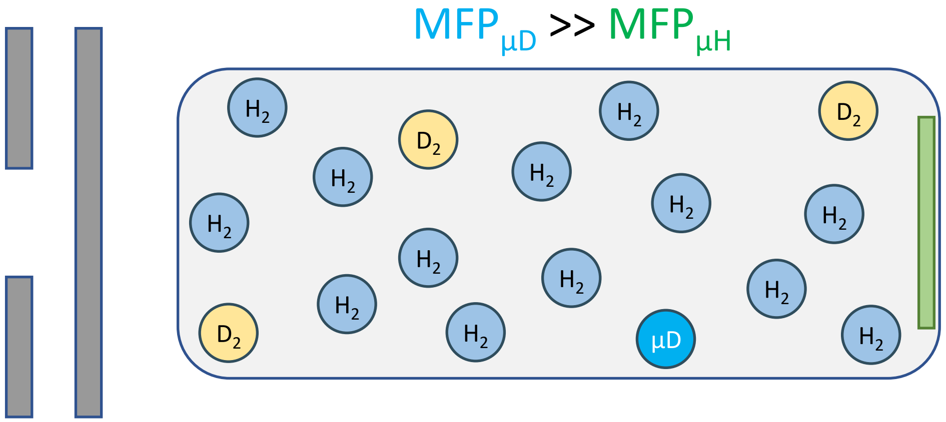

Bubak, M., & Fajman, M. P. (1987). Cross sections for hydrogen muonic atomic processes in two-level approximation of the adiabatic framework (No. JINR-E--4-87-464). Joint Inst. for Nuclear Research.
Adamczak, Andrzej, et al. "Muonic atom spectroscopy with microgram target material." The European Physical Journal A ***59*** *(2023): 15.*

Measuring microgram materials

Traditionally: Limited to target mass O(10-100 mg)

Hydrogen gas cell (100 bars; 0.25% deuterium)

- Limited to O(5 µg)
- Down to 20 year half-life (radioprotection)

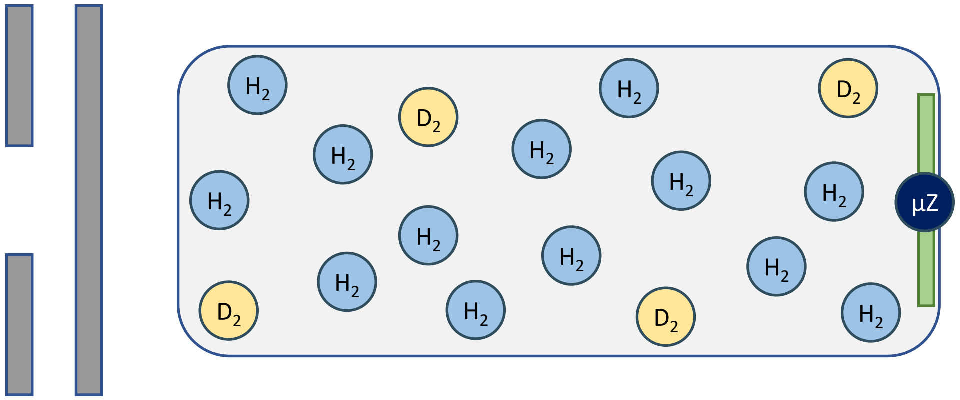

Bubak, M., & Fajman, M. P. (1987). Cross sections for hydrogen muonic atomic processes in two-level approximation of the adiabatic framework (No. JINR-E--4-87-464). Joint Inst. for Nuclear Research.

Adamczak, Andrzej, et al. "Muonic atom spectroscopy with microgram target material." The European Physical Journal A ***59*** *(2023): 15.*

Measuring microgram materials

Traditionally: Limited to target mass O(10-100 mg)

Hydrogen gas cell (100 bars; 0.25% deuterium)

- ➢Limited to O(5 µg)
- ➢Down to 20 year half-life (radioprotection)

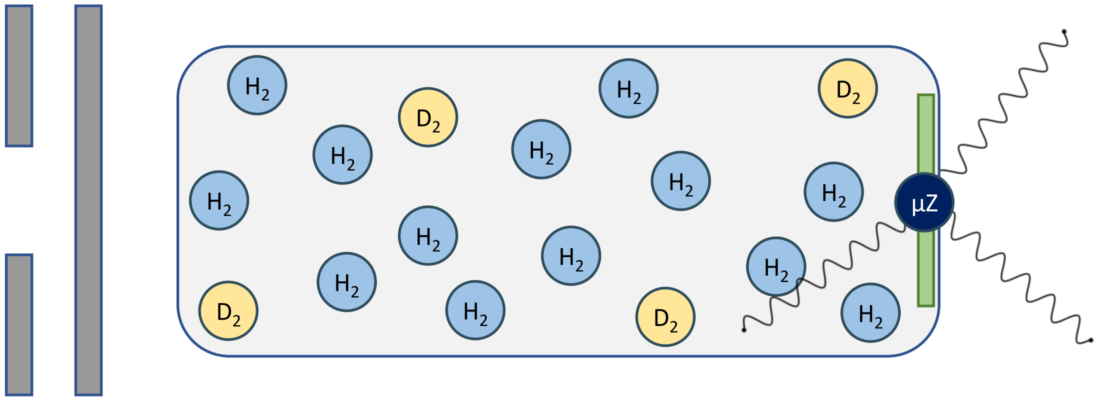

Bubak, M., & Fajman, M. P. (1987). Cross sections for hydrogen muonic atomic processes in two-level approximation of the adiabatic framework (No. JINR-E--4-87-464). Joint Inst. for Nuclear Research.

Adamczak, Andrzej, et al. "Muonic atom spectroscopy with microgram target material." The European Physical Journal A **59** (2023): 15.

μ-atomic spectroscopy with muX at PSI

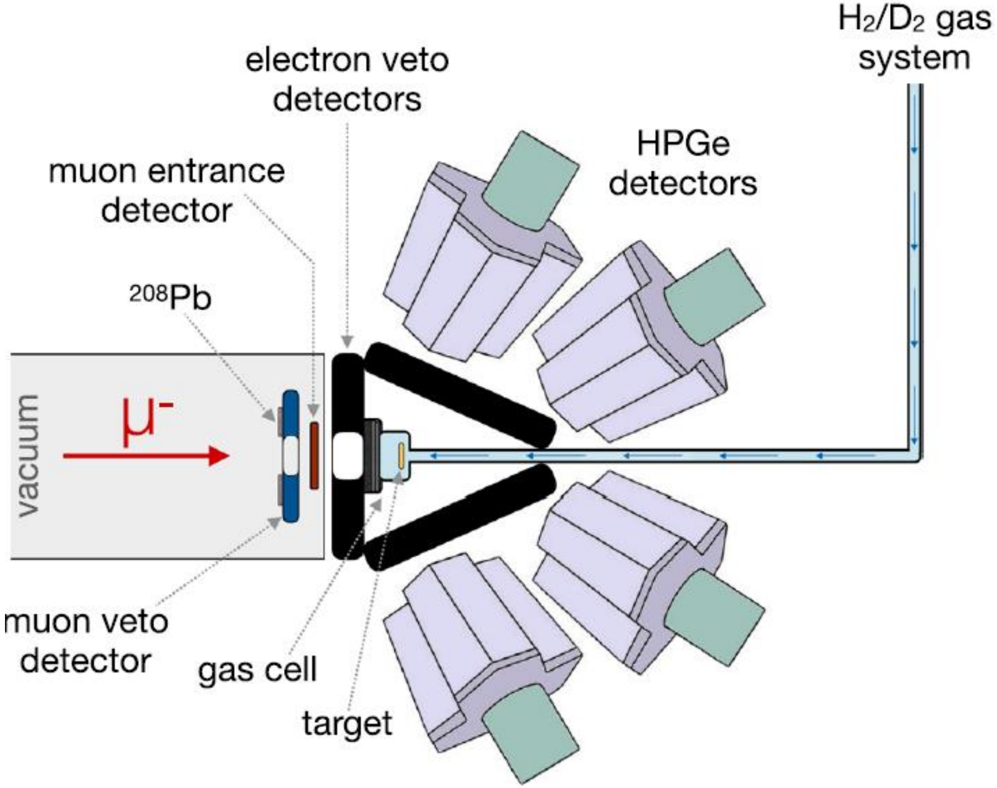

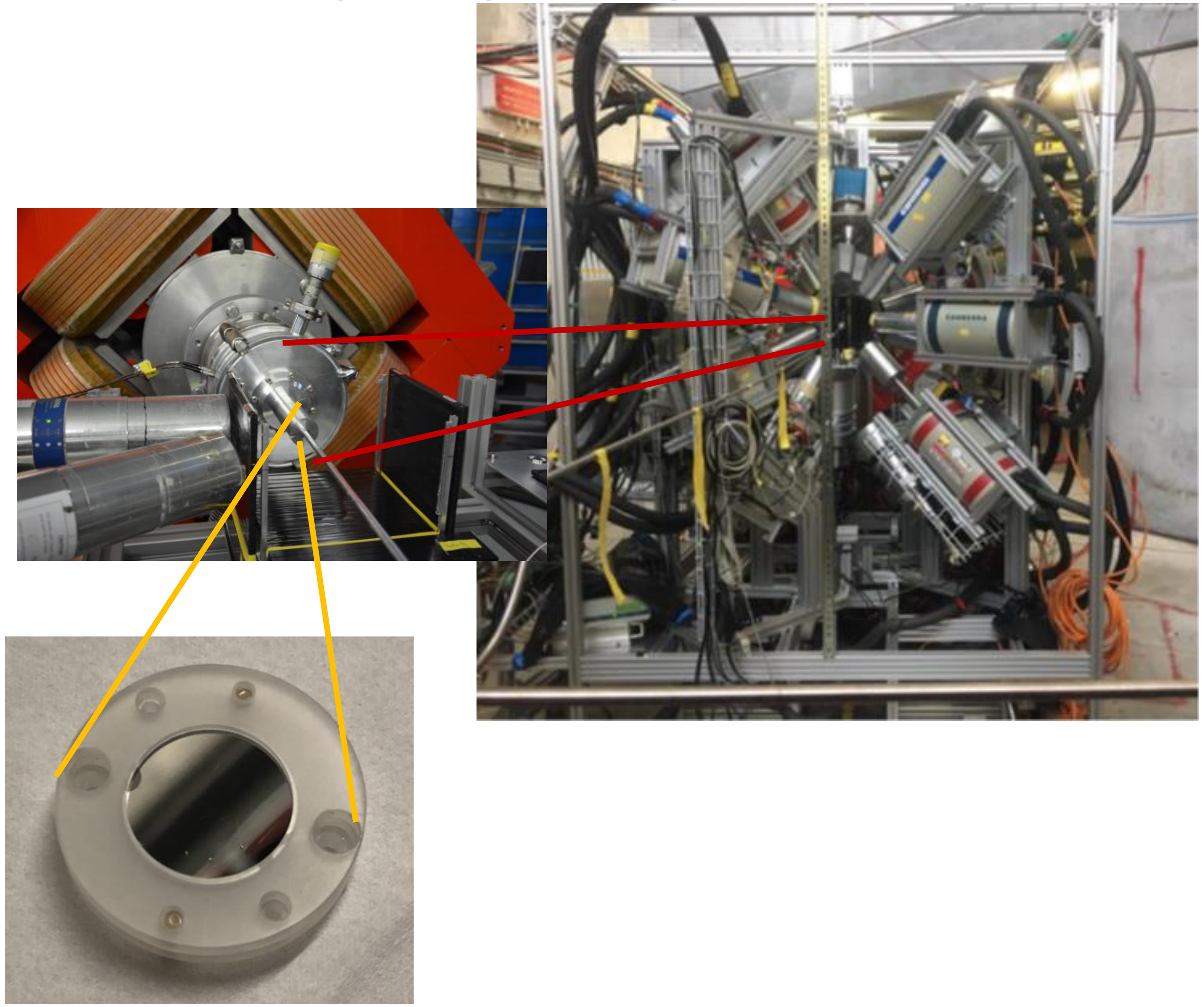

A. Adamczak et al., Muonic atom spectroscopy with microgram target material, Eur. Phys. A ***59*** *(2023) 15.*

Progress:
The 2023 & 2024 campaigns

2023: ^{39,40,41}K and ^{35,37}Cl

- Large targets for ^{39,41}K and ^{35,37}Cl
  → Direct stopping with high statistics
  Uncertainty dominated by calibration error.
  ➔ 2p1s, 3p1s, and 4p1s energies extracted with ~15-25 eV precision

- Small target for ^{40}K (~10 µg)
  → muX transfer mechanism with limited statistics
  Uncertainty dominated by statistical error.
  ➔ 2p1s energy extracted with ~35 eV precision

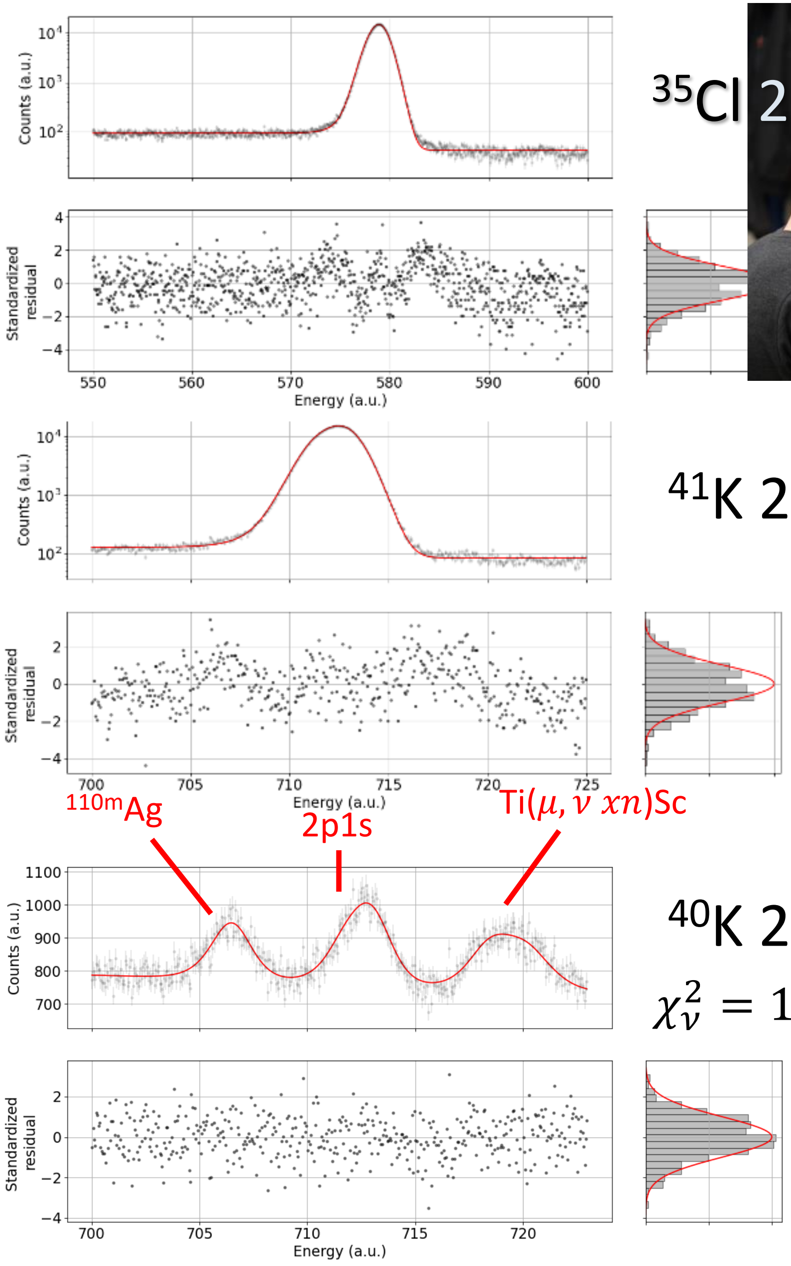

 PhD work Michael Heines (KU Leuven).

2024 campaign

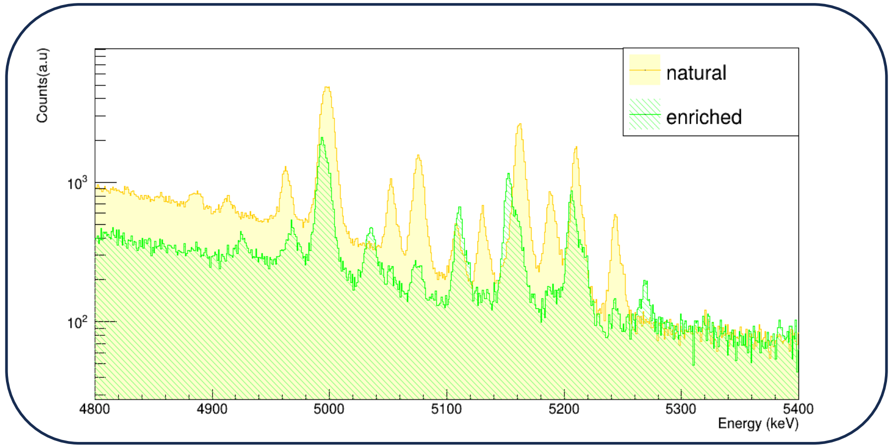

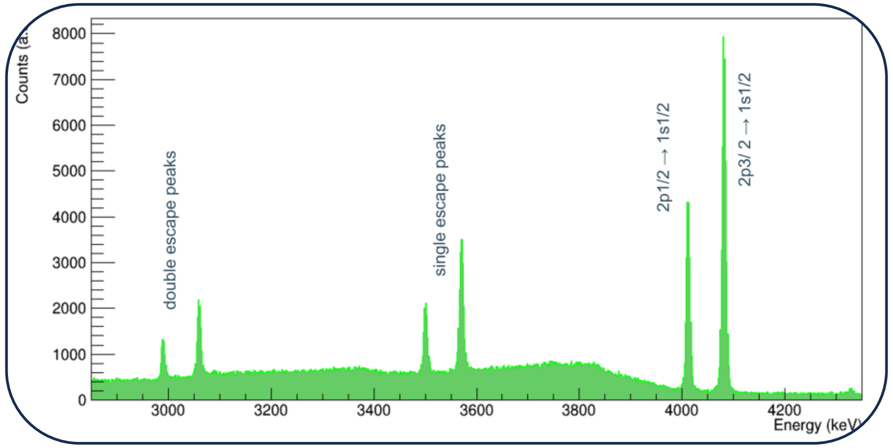

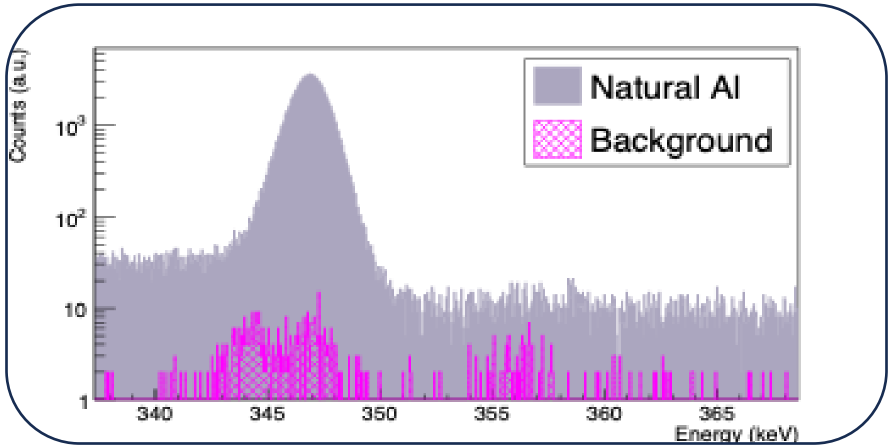

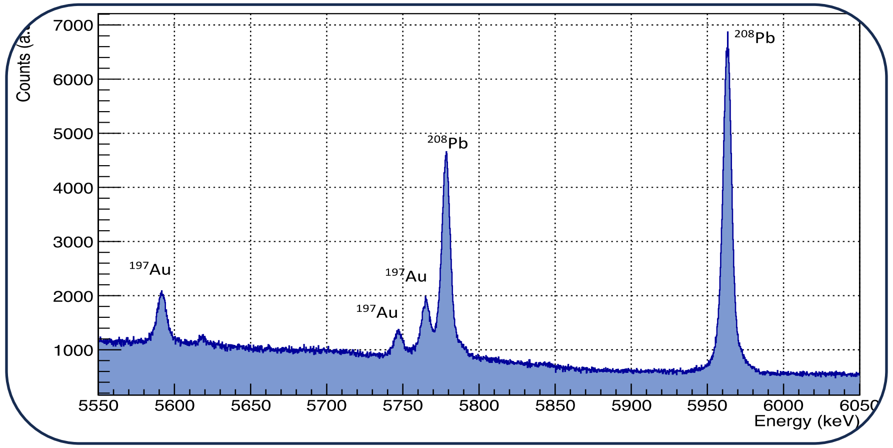

^{175,176}Lu

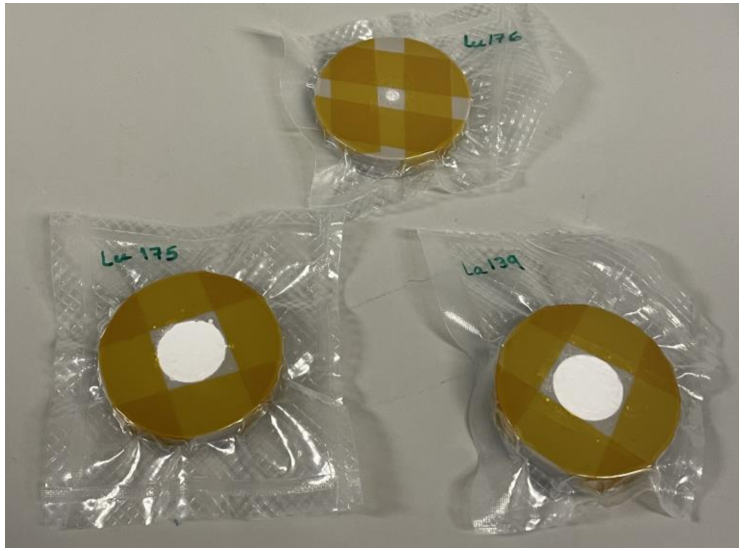

Input for laser spectroscopy experiment at CERN (IS773).

No isotopically pure samples

- ^{nat}Lu (97.4% ^{175}Lu vs 2.6% ^{176}Lu)
- ^{enr}Lu (25% ^{175}Lu vs 75% ^{176}Lu)

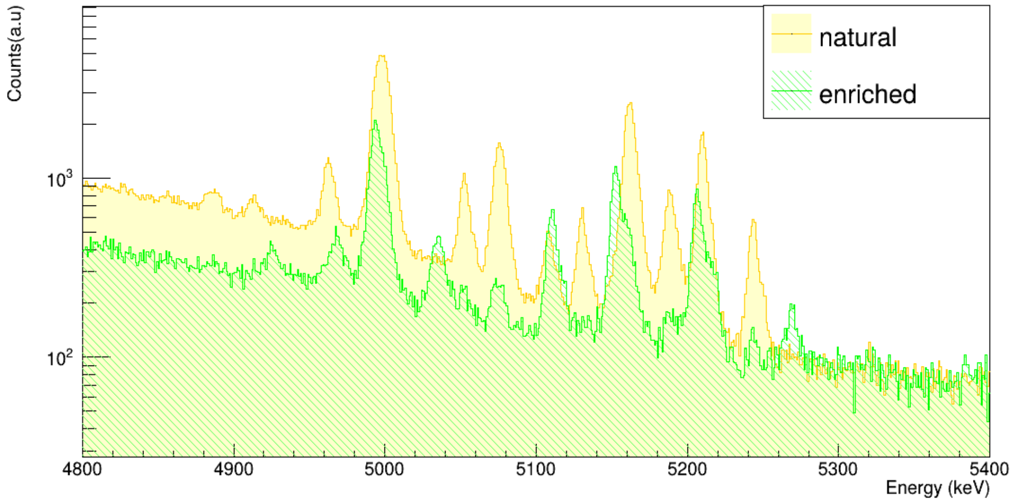

High quadrupole moment resulting in not only fine + hyperfine splitting but also DYNAMIC hyperfine splitting, including contribution from excited nuclear states.

Complex analysis ahead but data quality is really good.

PhD work War War Myint Myat Phyo (KU Leuven).

^{139}La

Initial test with ^{nat}La in preparation for this year's campaign.

^{nat}La is mostly made of ^{139}La and provided a clear spectrum that demonstrates the readiness for this measurement.

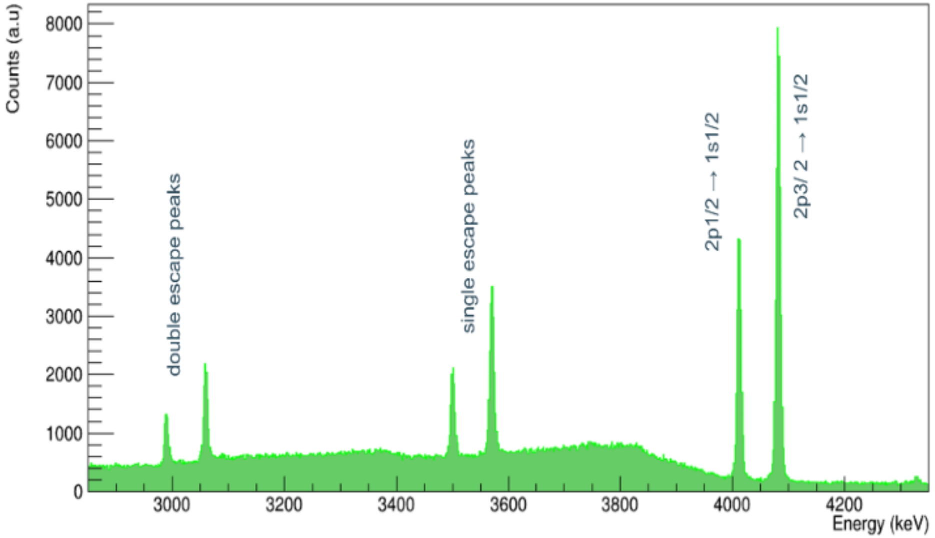

 PhD work War War Myint Myat Phyo (KU Leuven).

^{27}Al & ^{28,29,30}Si

In preparation for a future campaign on ^{26}Al, we investigated the suitability of the technique in that mass region.

- Muonic x-ray spectroscopy of ^{27}Al as a proof of principle and to compare with a targe-free measurement.
- Measurement of ^{28,29,30}Si with enriched targets to demonstrate the achievable precision.

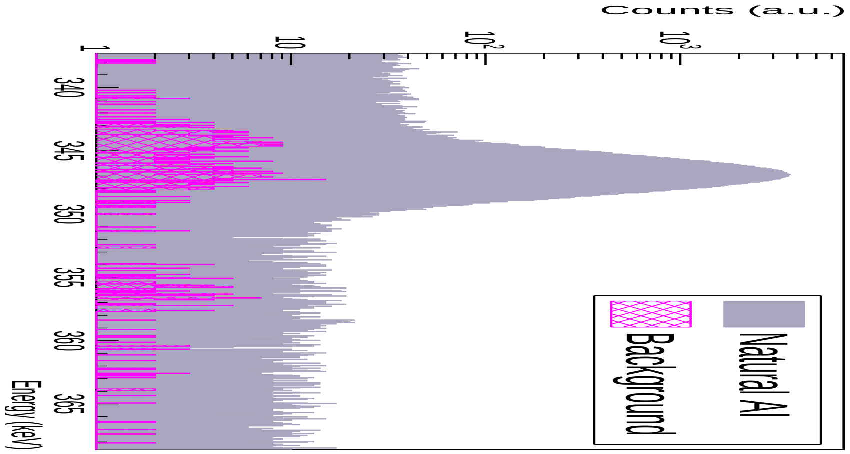

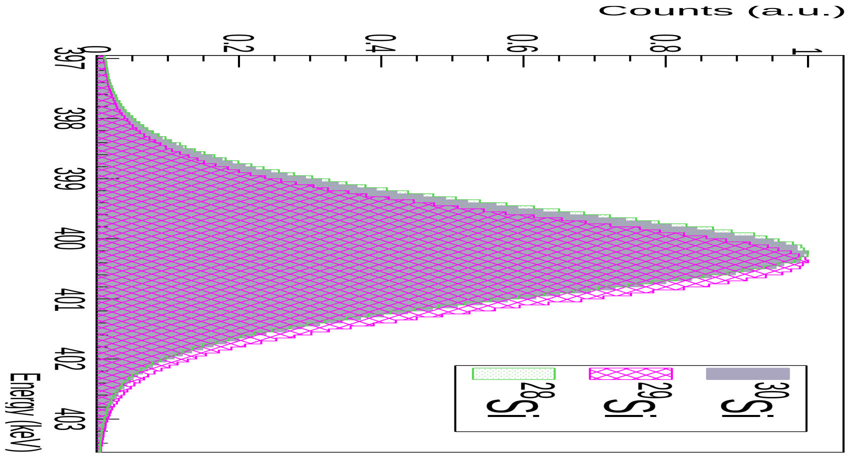

PhD work Marie Deseyn (KU Leuven).

Pb-Au-H_2O

^{208}Pb and ^{197}Au are reference isotopes that we use when investigating high-energy muonic x-ray.

Recently, the energy of those lines were challenged, especially with respect to the calibration lines used in the original measurement.

A new investigation was made, using a muon-capture line in ^{16}O at high energy to ensure future proper calibrations.

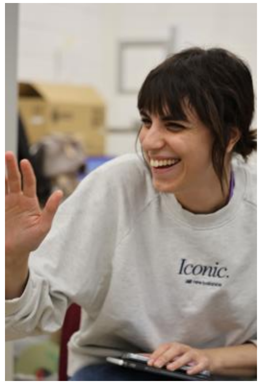

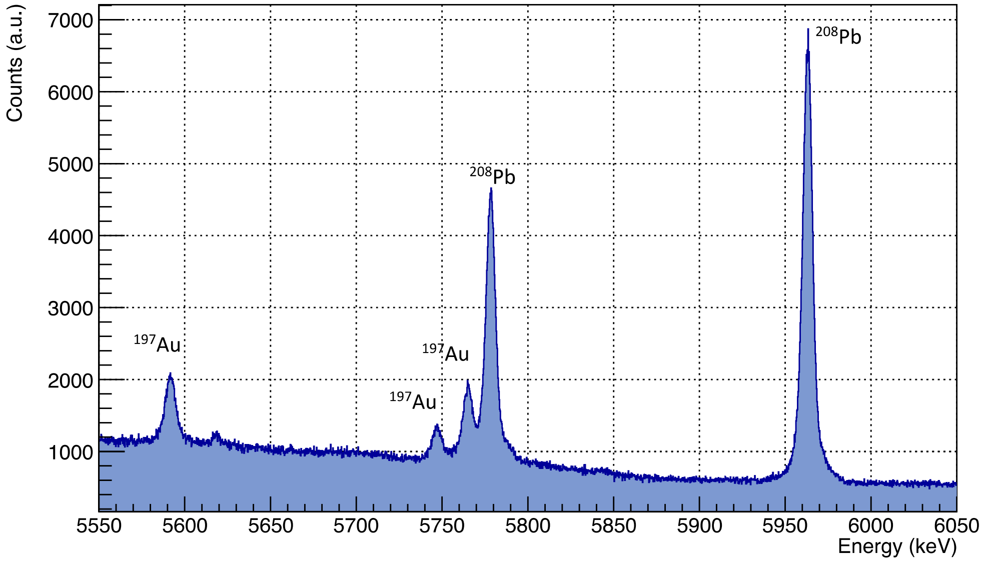

PhD work Anastasia Doinaki (PSI/ETH Zurich).

2025 Request

$^{137,138,139}La$

^{114}La is a proton-emitting nucleus predicted to have a strong prolate deformation – complementary to ^{151}Lu, which has a slight oblate deformation.

Comparing their charge radius evolution will allow to disentangle the contribution from deformation to that from the unbound proton.

We seek to measure 3 absolute charge radii to benchmark the laser spectroscopy.

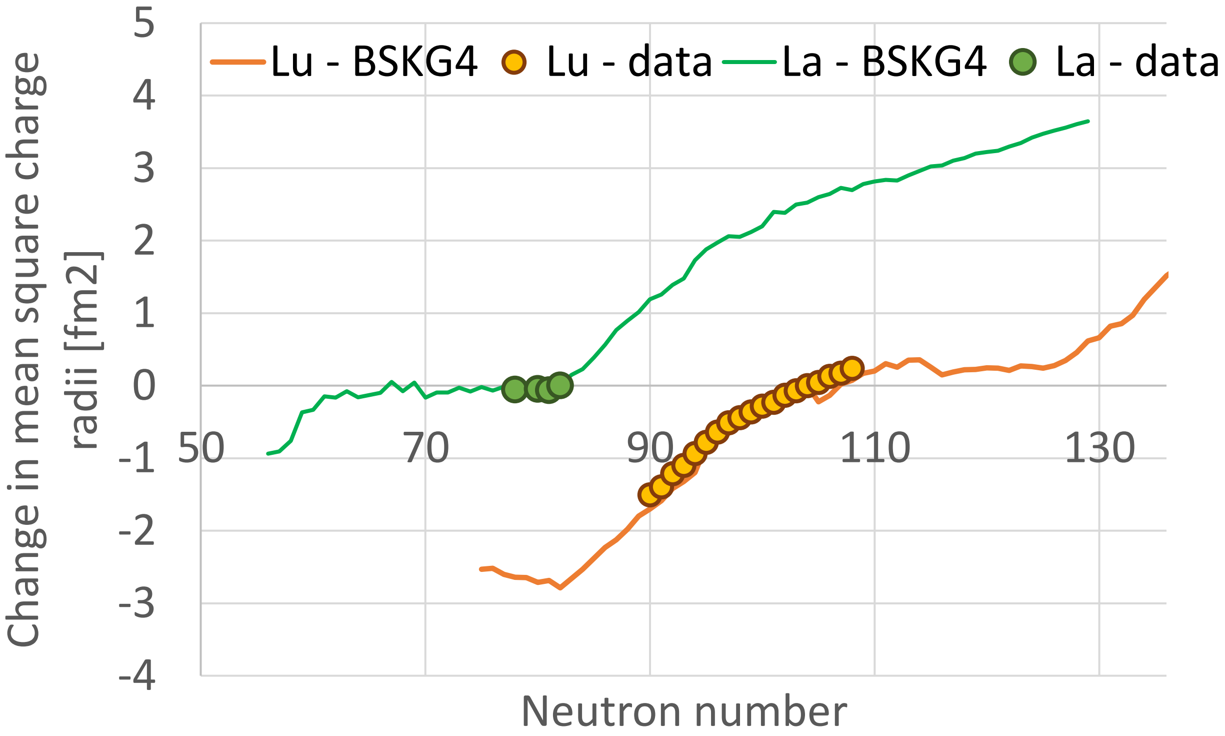

KU LEUVEN 600

^{137,138,139}La – Target readiness

- ^{139}La is naturally abundant and can be used directly, as shown in 2024.
- ^{137}La is readily available from a Mössbauer spectroscopy group in Poland. The target should be reconditioned at PSI prior to the beam time.
- ^{138}La will be separated from a pre-enriched sample at the RISIKO mass separator in Mainz.

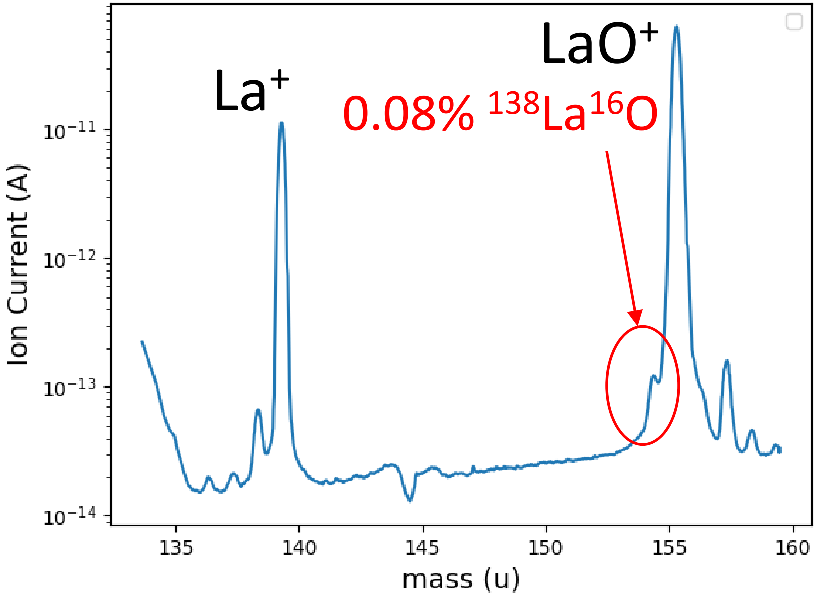

✓ Achieved 1.5% efficiency with surface ionized LaO^+ at test beam time in October 2024.

✓ Full sample preparation planned in spring 2025 ➔ 8.8 µg sample with >99% purity.

KU LEUVEN 600

$^{137,138,139}La$ – Request

- Given the small samples for $^{137,138}La$, we shall use the muon transfer approach in the high-pressure gas cell. ➔ 4+6 days
- ^{139}La will be limited by the systematic of the energy calibration ➔ 1 day
- We require 2 to 3 days to setup the array and gas cell and 1 day to calibrate the array.
- If not running following MIXE, 1 additional week will be required to install GIANT in PiE1.

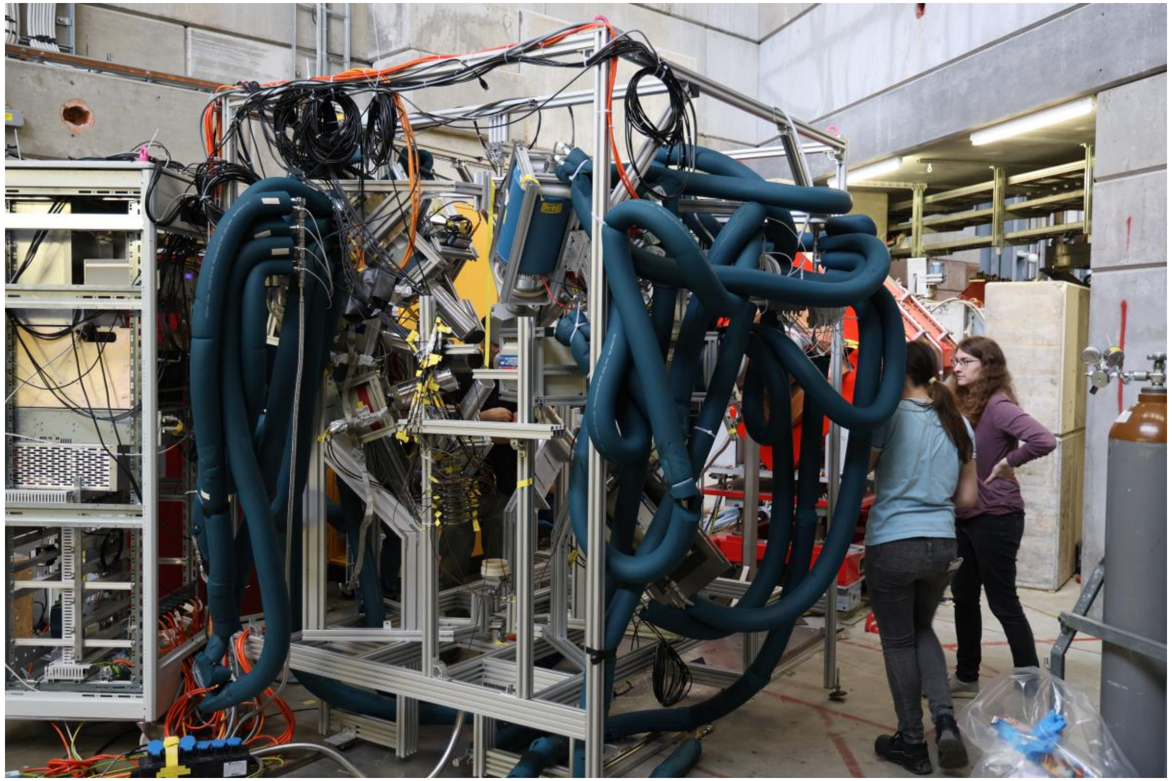

KU LEUVEN

- Reference Radii has a broad program, determining absolute charge radii from Al to Th, supporting research in nuclear structure and fundamental interactions.
- The 2023 and 2024 campaigns have been very successful, providing data on $^{28,29,30}Si$, $^{35,37}Cl$, $^{39,40,41}K$, and $^{175,176}Lu$, contributing to this scientific program.
- The data analysis is progressing and we are about to release our first results on $^{35,37}Cl$, with many other publications in preparation (e.g., N=20 isotones, $_{19}K$ isotopic chain)
- For 2025, we are requesting **2 weeks** of beam time to measure the **^{137,138,139}La isotope triplet**.
- For 2026, we plan to bring the ISOLDE Decay Station HPGe array to support the study of most challenging cases for muX & RefRad.

Thank you!

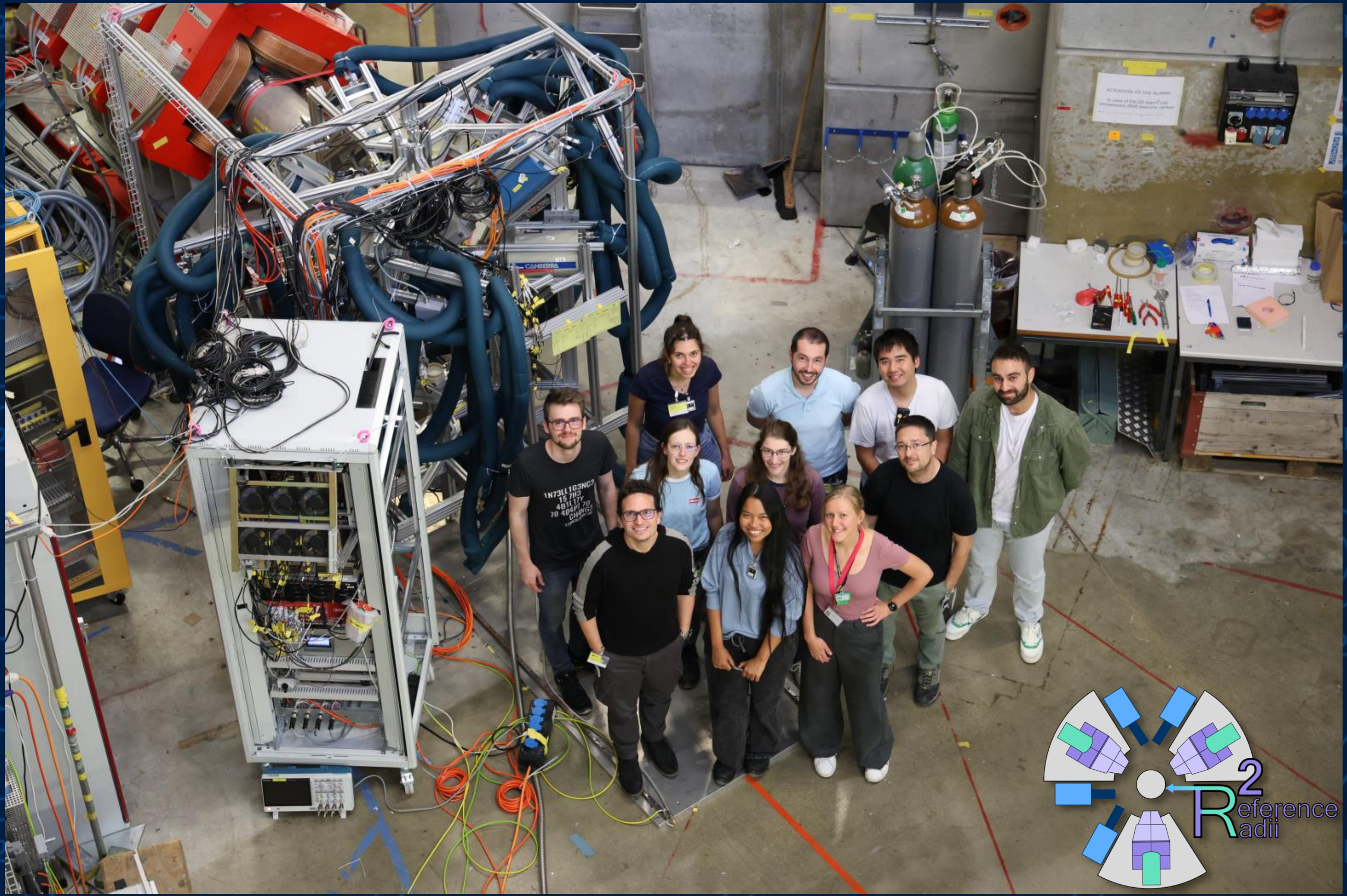

S. Bara[1], T.E. Cocolios[1], C. Costache[2], M. Deseyn[1], A. Doinaki[3,4], O. Eizenberg[5], Harshithbabu[1], M. Heines[1], A. Herzáň[6], A. Knecht[3], U. Köster[7], R. Licá[2], R. Mancheva[1,8], V. Matoušek[6], E. Maugeri[3], M. Niikura[9], B. Ohayon[5], A. Ouf[10], W.W.M.M Phyo[1], R. Pohl[10], N. Ritjoho[11], J. Shaw[1], A. Turturica[2], S.M. Vogiatzi[1], K. von Schoeler[3,4], F. Wauters[10], W. Wojtaczka[1], and A. Zendour[3,4]

[1]KU Leuven, Belgium
[2]IFIN-HH, Bucharest, Romania
[3]Paul Scherrer Institut, Villigen, Switzerland
[4]ETH Zürich, Switzerland
[5]Technion—IIT, Israel
[6]Slovak Academy of Sciences, Slovakia
[7]Institut Laue-Langevin, France
[8]CERN, Geneva, Switzerland
[9]RIKEN Nishina Center, Japan
[10]Johannes Gutenberg University Mainz, Germany
[11]Suranaree University of Technology, Nakhon Ratchasima, Thailand

Back up:
Radius extraction

Energy calibration for K and Cl

Non-parametric bootstrapping → Calibration error prediction

Average over detectors to improve uncertainty and reliability

Bias when averaging detectors (shared FPGa/digitizers)
→ ~8 eV bias

Several detectors with ~10 eV calibration error

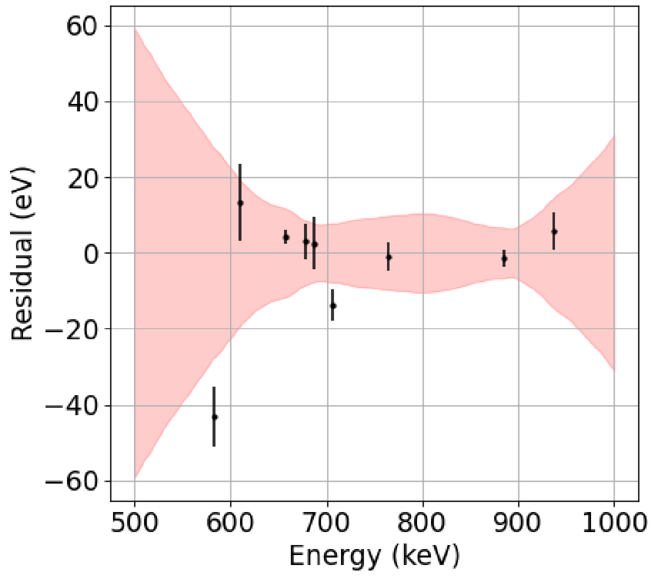

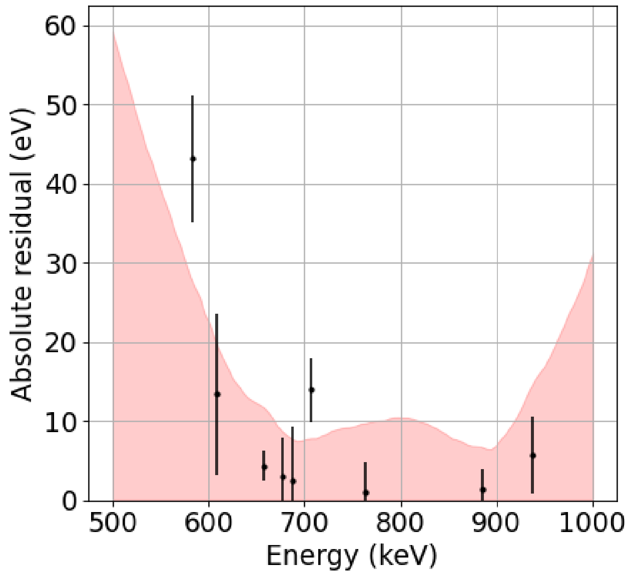

Radius extraction – General concept

Finite size correction scales with $\frac{1}{r^3} \approx 10^7$

Muonic x-ray energies more sensitive to charge radius

Calculate transition energy for many radii → Compare with experiment

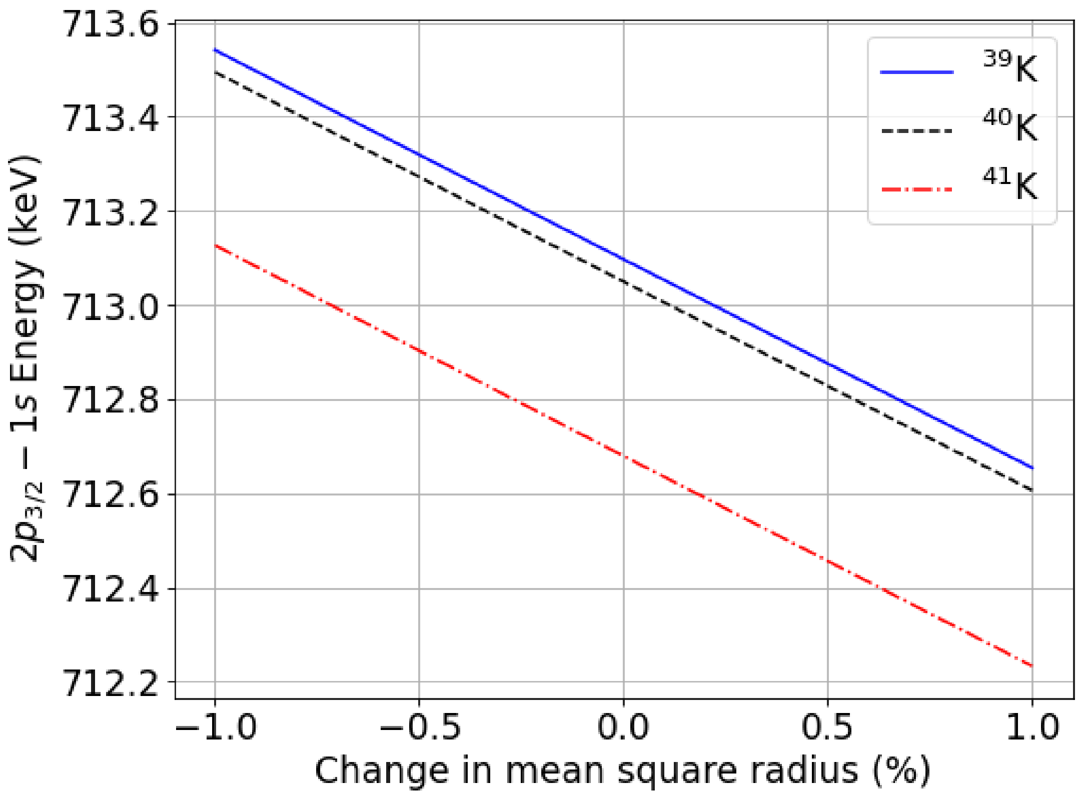

Simple calculations with mudirac code [1]

*Sturniolo, Simone, and Adrian Hillier. "Mudirac: A Dirac equation solver for elemental analysis with muonic X-rays." X-Ray Spectrometry **50** (2021) 180-196.*

Radius extraction – The shape of the nucleus

QED needs to assume nucleus:

$$\rho(r) = \frac{\rho_0}{1 + \exp\left(4\ln(3)\frac{r-c}{t}\right)}$$

Take t fixed (no sensitivity in experiment)

Variation of t changes $\sqrt{\langle r^2 \rangle}$

The Barret solution:

- Introduce Barret radius → Insensitive to t
- Combine with electron scattering to predicted radii in a combined analysis

$$\sqrt{\langle r^2 \rangle} = \frac{R^{\mu}_{k\alpha}}{V^{e}_{2}}$$

Radius extraction – The shape of the nucleus

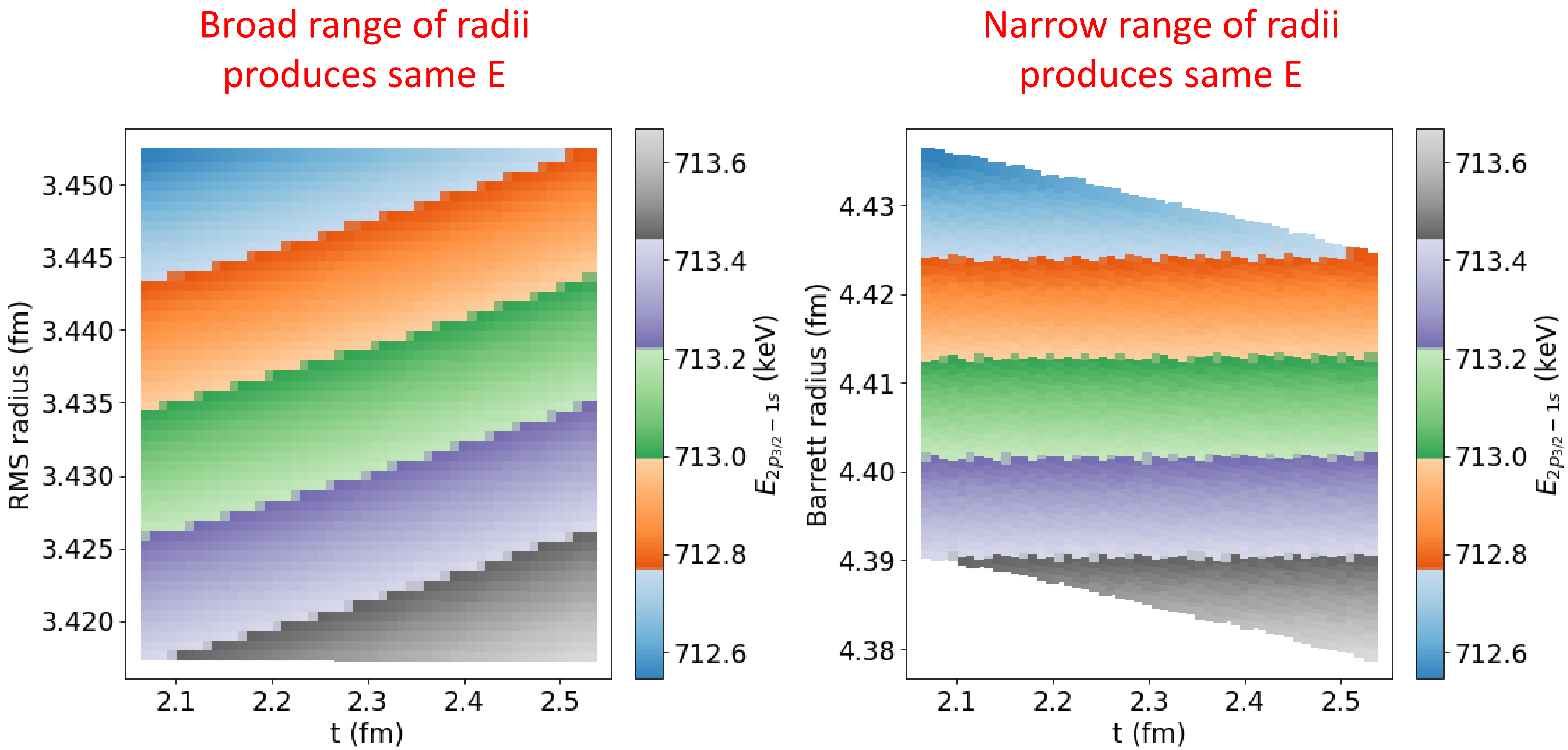

Simple calculations with mudirac code [1]

*Sturniolo, Simone, and Adrian Hillier. "Mudirac: A Dirac equation solver for elemental analysis with muonic X-rays." X-Ray Spectrometry **50** (2021) 180-196.*

Radius extraction – The shape of the nucleus

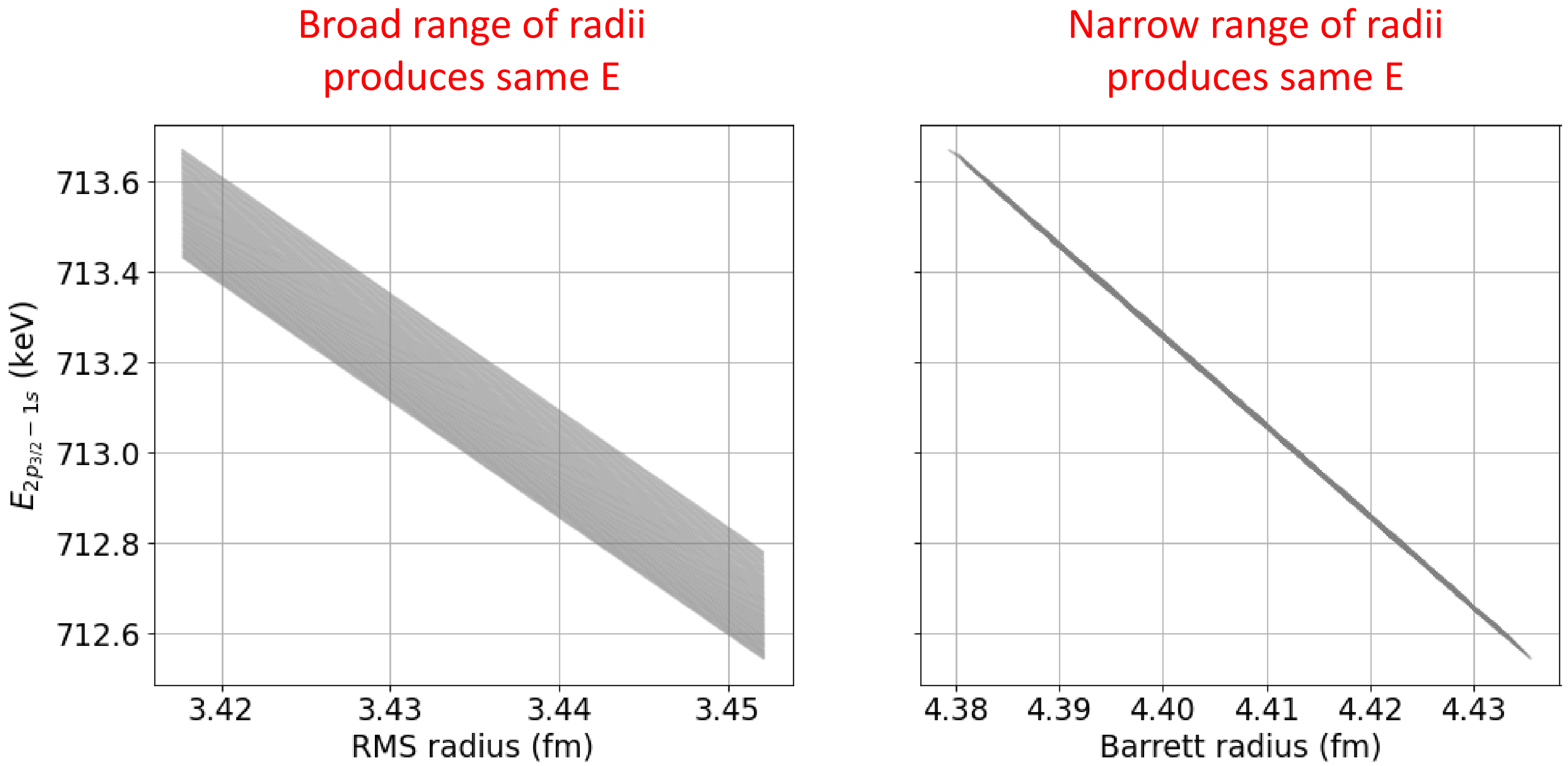

Simple calculations with mudirac code [1]

Sturniolo, Simone, and Adrian Hillier. "Mudirac: A Dirac equation solver for elemental analysis with muonic X-rays." X-Ray Spectrometry ***50*** *(2021) 180-196.*

Radius extraction – What is really needed?

Transition energies ✓

Theory

- QED → Ongoing
- Nuclear polarization → Finalizing

V_2 correction:

- Available scattering for ^{39}K and $^{35,37}Cl$ ✓
- Calculations for $^{40,41}K$ → Ongoing

KU LEUVEN 600

Field-theoretical approach

$$\hat{J}^{\mu}_{\mathrm{N,\,total}}(x) = J^{\mu}_{\mathrm{N,\,stat}}(\mathbf{x}) + \hat{J}^{\mu}_{\mathrm{N,\,fluc}}(x)$$

$$\hat{A}^{\mu}_{\mathrm{total}}(x) = \mathcal{A}^{\mu}_{\mathrm{stat}}(\mathbf{x}) + \underbrace{\hat{A}^{\mu}_{\mathrm{fluc}}(x) + \hat{A}^{\mu}_{\mathrm{free}}(x)}_{:= \hat{A}^{\mu}_{\mathrm{rad}}(x)}$$

$$iD_{\mu\nu}(x - x') = \langle 0|T[\hat{A}^{\mathrm{free}}_{\mu}(x)\hat{A}^{\mathrm{free}}_{\nu}(x')]|0\rangle$$

dressed muon propagator

modified photon propagator:

$$i\mathcal{D}_{\mu\nu}(x, x') = \langle 0|T[\hat{A}^{\mathrm{rad}}_{\mu}(x)\hat{A}^{\mathrm{rad}}_{\nu}(x')]|0\rangle$$

$$= iD_{\mu\nu}(x - x') + \langle 0|T[\hat{A}^{\mathrm{fluc}}_{\mu}(x)\hat{A}^{\mathrm{fluc}}_{\nu}(x')]|0\rangle$$

Modified photon propagator

$$\mathcal{D}_{\mu\nu}(x,x') = D_{\mu\nu}(x-x') + D^{\mathrm{NP}}_{\mu\nu}(x,x')$$

NP tensor

"seagull" term

$$D^{\mathrm{NP}}_{\mu\nu}(x,x') = \int d^4x_1\, d^4x_2\, D_{\mu\xi}(x-x_1) \left[\Pi^{\xi\zeta}_{\mathrm{N}}(x_1,x_2) + S^{\xi\zeta}_{\mathrm{N}}(x_1,x_2)\right] D_{\zeta\nu}(x_2-x')$$

$\mathcal{D}_{\mu\nu}(x,x') =$

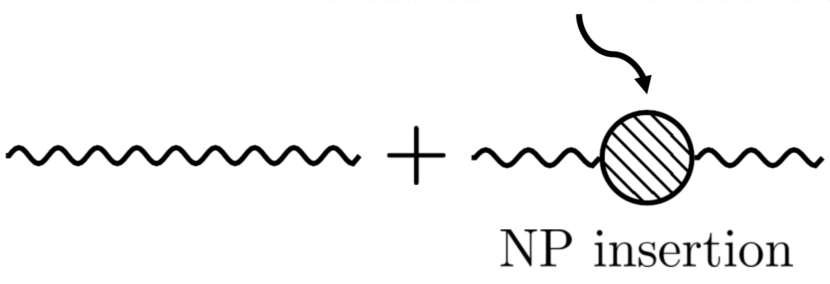

$$i\Pi^{\xi\zeta}_{\mathrm{N}}(x_1,x_2) = \langle 0|T[\hat{J}^{\xi}_{\mathrm{N,\,fluc}}(x_1)\hat{J}^{\zeta}_{\mathrm{N,\,fluc}}(x_2)]|0\rangle$$

Slide courtesy: Igor Valuev

What is needed from the nuclear side

$$\mathrm{NP} \to \sum_{|\lambda\rangle} [\text{the entire nuclear spectrum}]$$

- excitation energies $\omega_\lambda = E_\lambda - E_0$
- reduced matrix elements:
  - transition (charge) densities
    $\varrho_J^\lambda(\mathrm{x}) = \langle \lambda || \int d\Omega_{\mathbf{x}}\, Y_J(\Omega_{\mathbf{x}}) \hat{\rho}_{\mathrm{N}}(\mathbf{x}) || 0 \rangle$
  - transition current densities
    $\mathcal{J}_{JL}^\lambda(\mathrm{x}) = \langle \lambda || \int d\Omega_{\mathbf{x}}\, \mathbf{Y}_{JL}(\Omega_{\mathbf{x}}) \cdot \hat{\mathbf{J}}_{\mathrm{N}}(\mathbf{x}) || 0 \rangle$

  for different excitation modes:
  $0^+, 1^-, 2^+, 3^-, (4^+, 5^-, 1^+)$
  in the laboratory frame

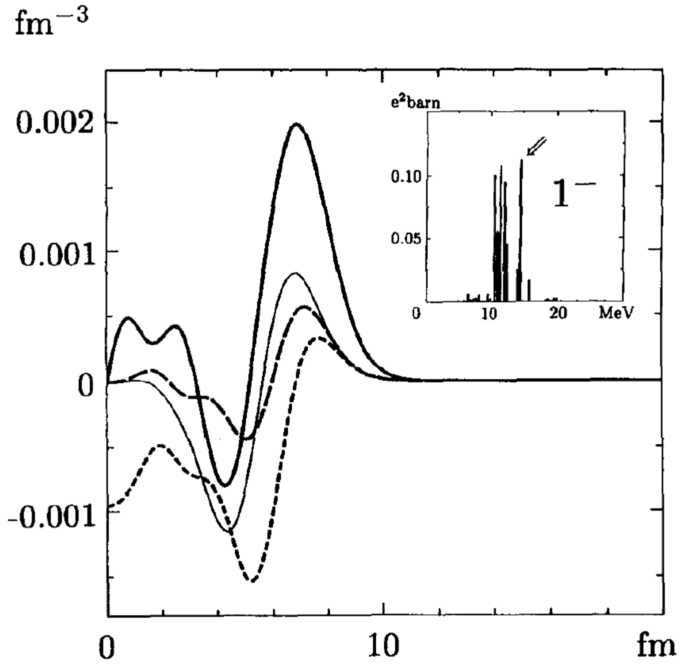

Y. Tanaka and Y. Horikawa, Nucl. Phys. A580, 291 (1994).

*simplifications are possible in terms of transition probabilities $B(EL)$

KU LEUVEN

Back up:
Progress on Ag

Muonic x-ray spectroscopy on Ag

Line	Energy (keV)	Sigma_exp (eV)	Sigma_bias (eV)	Sigma_lit (eV)	Sigma_tot (eV)
^{109}Ag - 2p3/2 - 1s	3177.325	92	253	1.9	346.9
^{109}Ag - 2p1/2 - 1s	3140.246	96	253	1.9	350.9
^{107}Ag - 2p3/2 - 1s	3184.429	62	189	1.9	252.9
^{107}Ag - 2p1/2 - 1s	3147.285	68	189	1.9	258.9

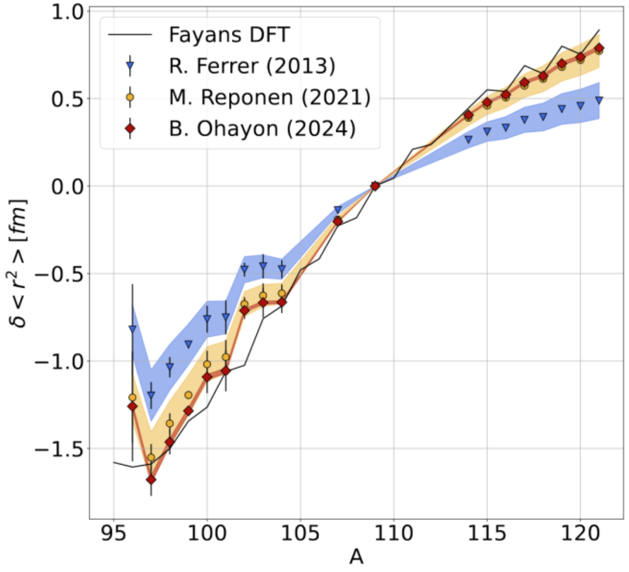

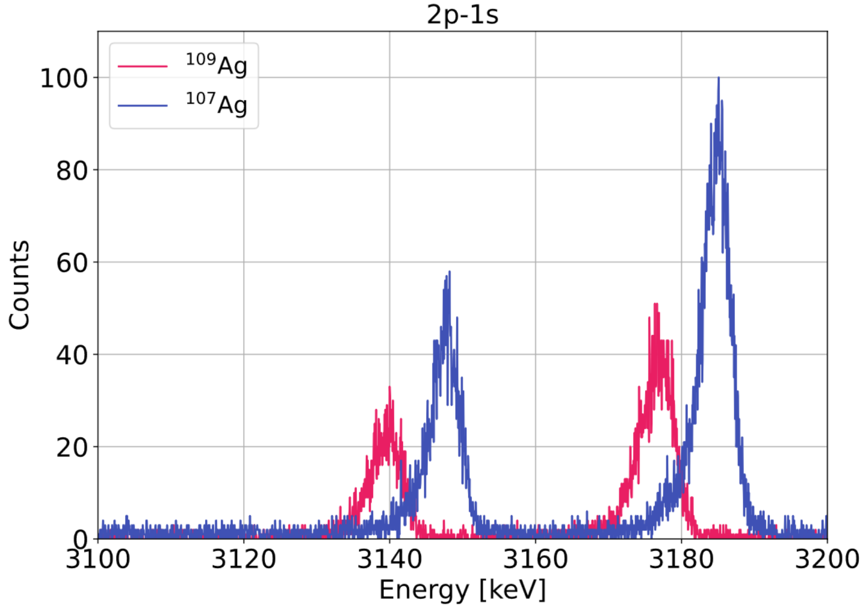

PhD work Marie Deseyn (KU Leuven).

^{108m}Ag BR2

Cycle I: 02/2025A: 18/03/2025 – 13/04/2025

Cycle II: 03/2025A: 13/05/2025 – 12/06/2025

Cycle III: 04/2025A: 03/07/2025 – 31/07/2025

Approximate activity at start of collection (ISOLDE)

- Activity Ag-108m @ “EOI”: 93 MBq
- Activity Ag-110m @ “EOI”: 1,53 GBq

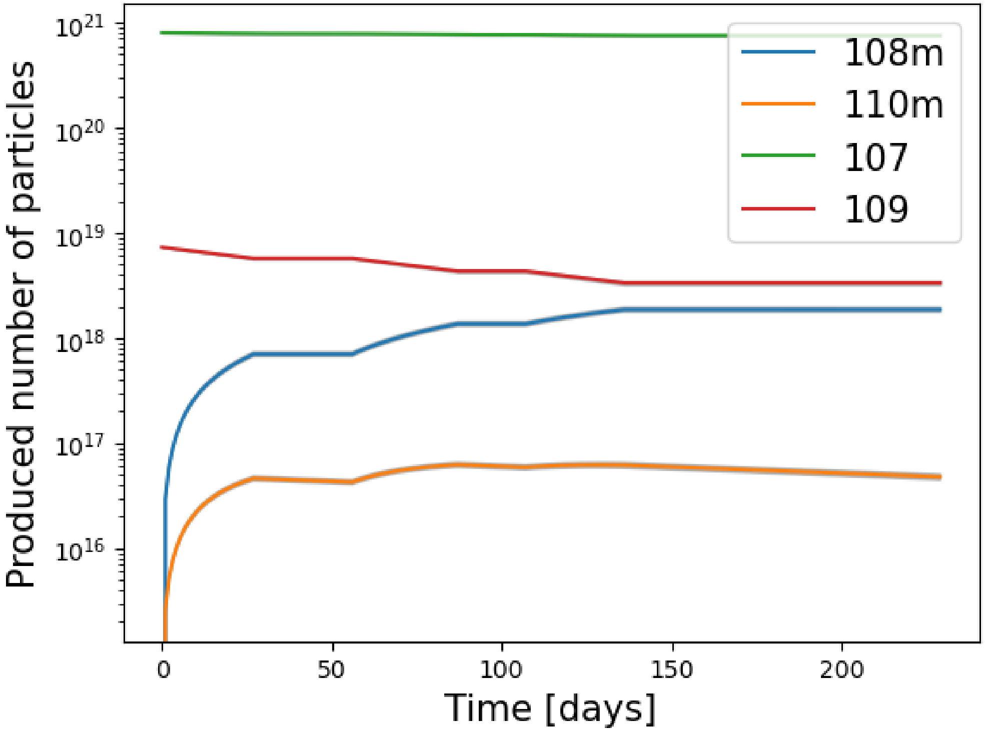

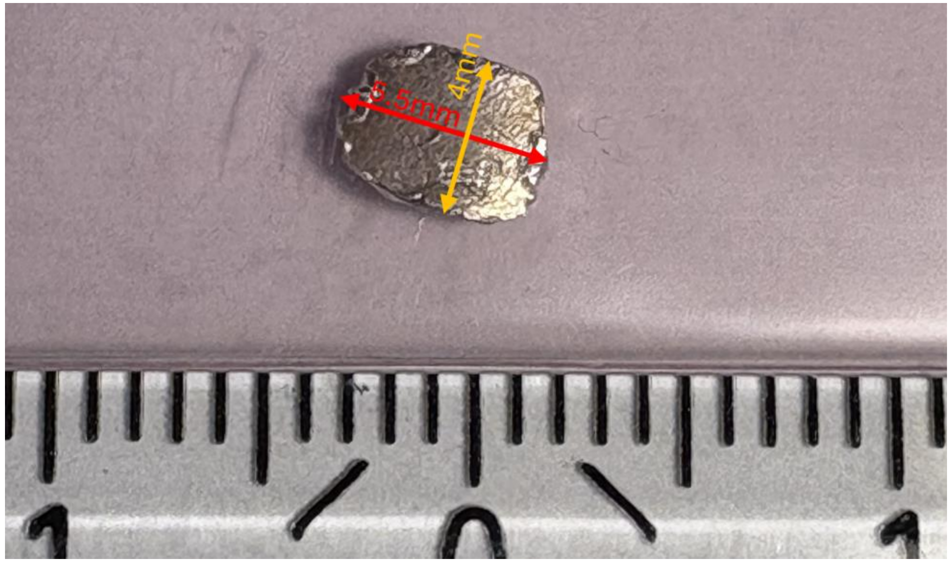

PhD work Marie Deseyn (KU Leuven).

^{108m}Ag collection

	Efficiency
on-resonance (based on GC2 data)	3.25(14)%
off-resonance (based on GC1 data)	1.21(12)%
off-resonance (based on GC3 data)	1.16(3)%

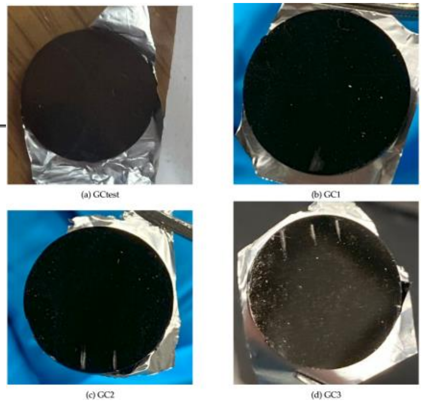

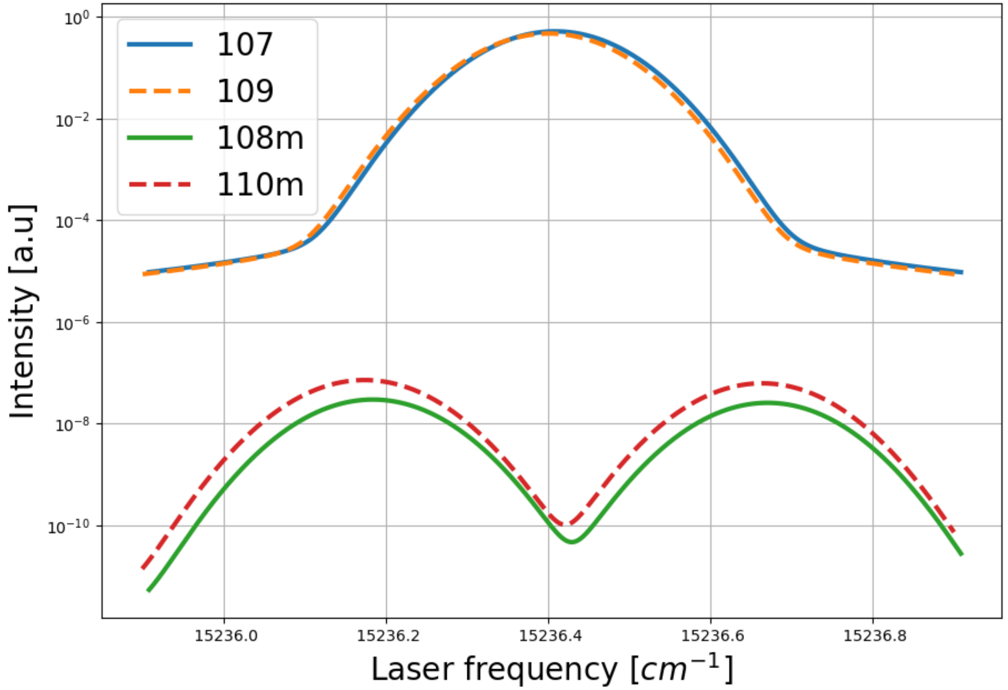

(a) Relative beam intensities as a function of wavelength of the first step laser. The green and blue lines correspond to ^{107}Ag and ^{109}Ag respectively, while the red and orange curves correspond to ^{108m}Ag and ^{110m}Ag respectively.

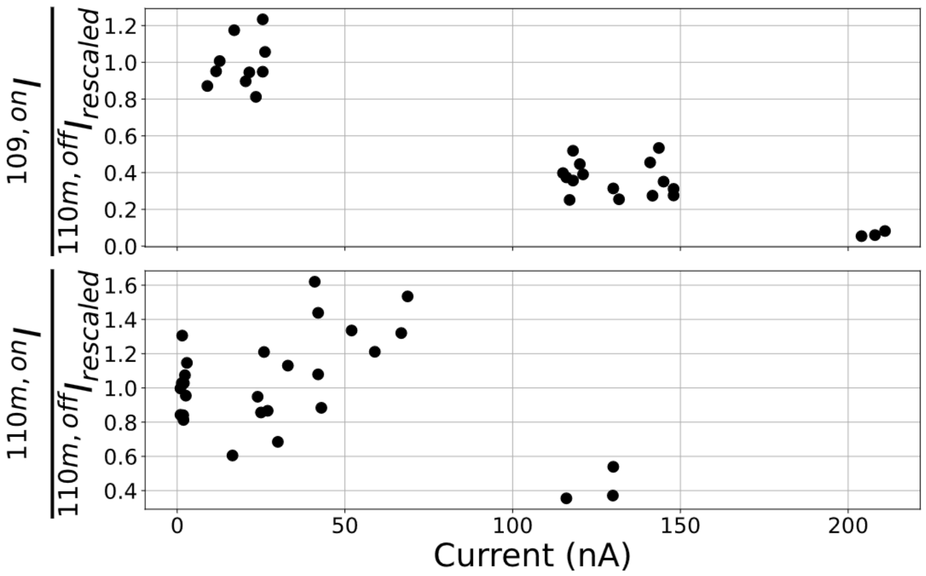

Figure 1: Beam current for lasers on the ^{109}Ag ($^{109,on}I$) and ^{110m}Ag ($^{110m,on}I$) resonance divided by the rescaled beam current for lasers off-resonance for ^{110m}Ag ($^{110m,off}I_{rescaled}$) as a function of $^{109,on}I$ and $^{110m,on}I$, respectively.

→ Implantation of 3.68 µg of ^{108m}Ag → Challenging measurement → Ideally with IDS array

Back up: ^{138}La target

^{138}La separation tests at RISIKO

Sample type :

Lanthanum nitrate solution, deposited on Zr foil

Efficiency of laser ionized La for different trial samples:

1) Only La on Zr foil : < 0.1 %
2) La on Zr foil, plus a few pieces of Y : ~ 0.5%
3) La+ Zr+ Y sandwich foil : ~ 0.5%

Mass scan over the full range shows that the surface ionized LaO is more efficient than

the laser ionized La

The temperatures for sample reservoir and ion source for the optimal ratio of LaO/La are investigated.

Under the optimal condition, efficiency of surface ionized LaO : ~ 1.5%

We will be able to implant 8.8 ug of ^{138}La.

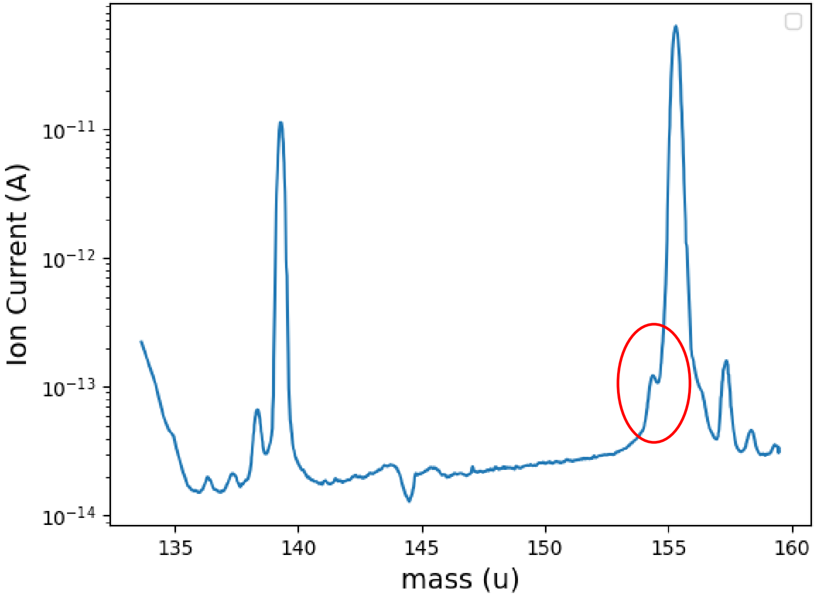

0.08% of ^{138}La in natural sample .

This will be more obvious in the enriched sample with 5.6% purity of ^{138}La .

Back up:
Progress Th
Plan Ac

Scientific case of actinides: ^{229,230,232}Th & ^{227}Ac

Indications towards strong octupole deformation have been observed for thorium and actinium; changes in the nuclear charge radii along the isotopic chain and hints for inverted odd-even staggering.

Muonic ^{232}Th spectrum from 2023 muX beam time

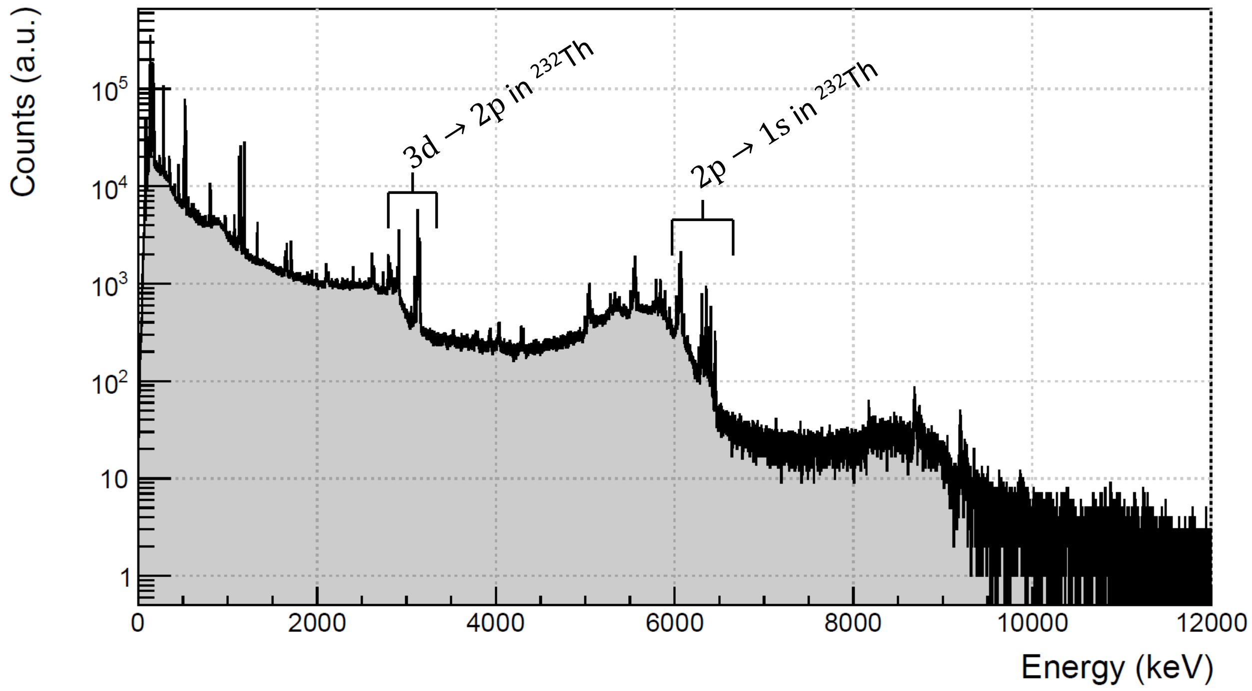

PRC 100, 044321 (2019)

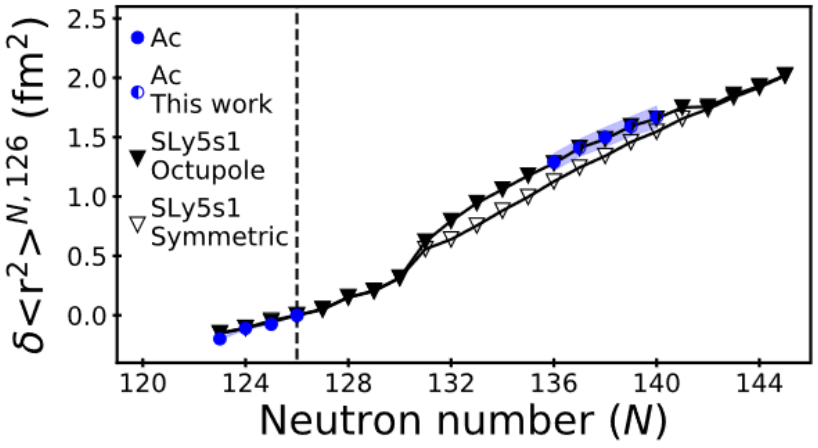

Strong octupole deformation in heavy mass isotopes can probe Beyond Standard Model (BSM) physics:

- Atomic Parity Violating (APV) effects in strongly octupole deformed isotopes are enhanced
- ^{229}Th nuclear clock is the best candidate to study variations of the fine structure constant

Feasibility of absolute nuclear charge radii measurement:

- ^{229,230,232}Th ($t_{1/2} \gg 10^3$ yrs)
- (?) ^{227}Ac ($t_{1/2} = 21.77$ yrs)

Postdoc work Stella Vogiatzi (KU Leuven).

Back up: V_{ud}

V_{ud}

Unitarity of CKM (matrix connects quark generations) = test of SM

V_{ud} = largest first-row element (mainly determined by superallowed $0^+ \rightarrow 0^+$ Fermi β decays)

Nuclear charge radius affects statistical rate function (f) and isospin-symmetry breaking correction (δC)

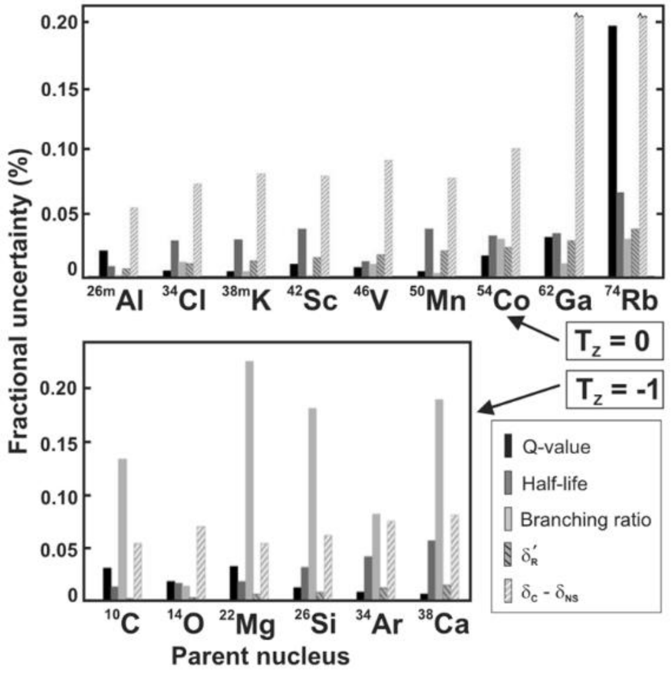

(a) For superallowed β-decays [26]

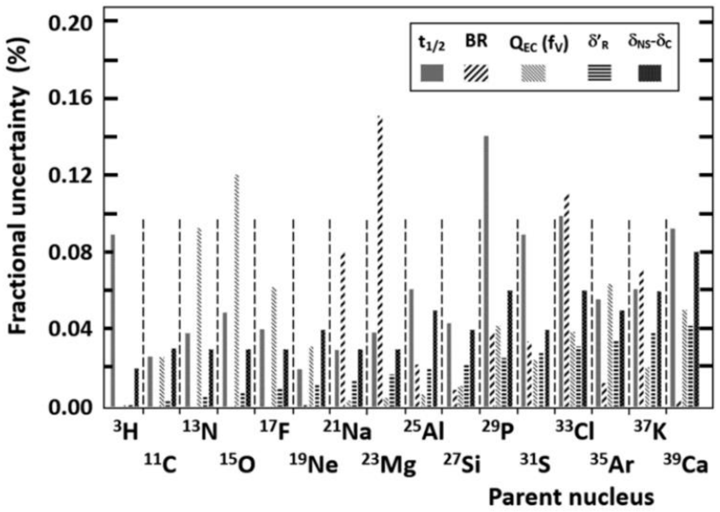

(b) For mirror transitions [19]

Back up: GEANT4

Geant4 simulation of GIANT array

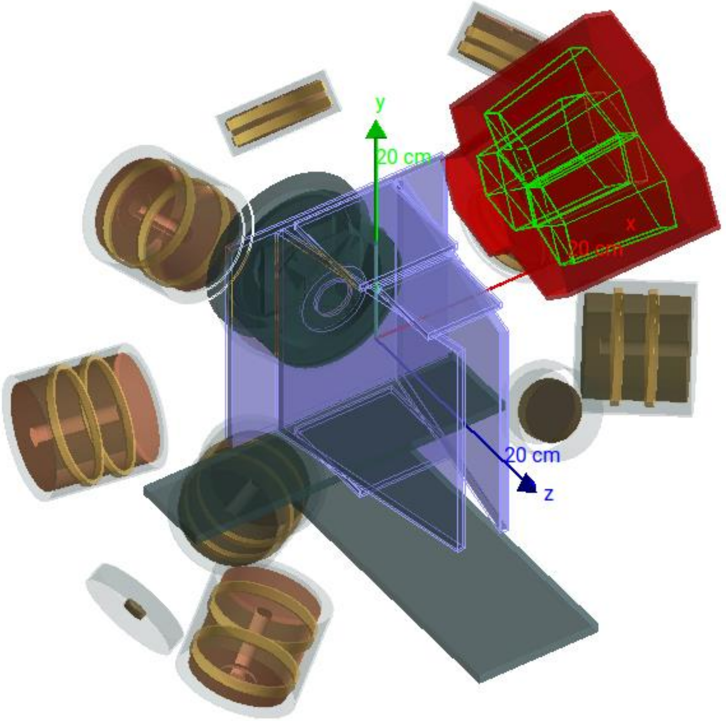

- Position optimization of detectors based on:
  - Statistics in peak of interest
  - Background coming from Bremsstrahlung
  - Allowed for quick online decisions
- Benchmark of the simulation:

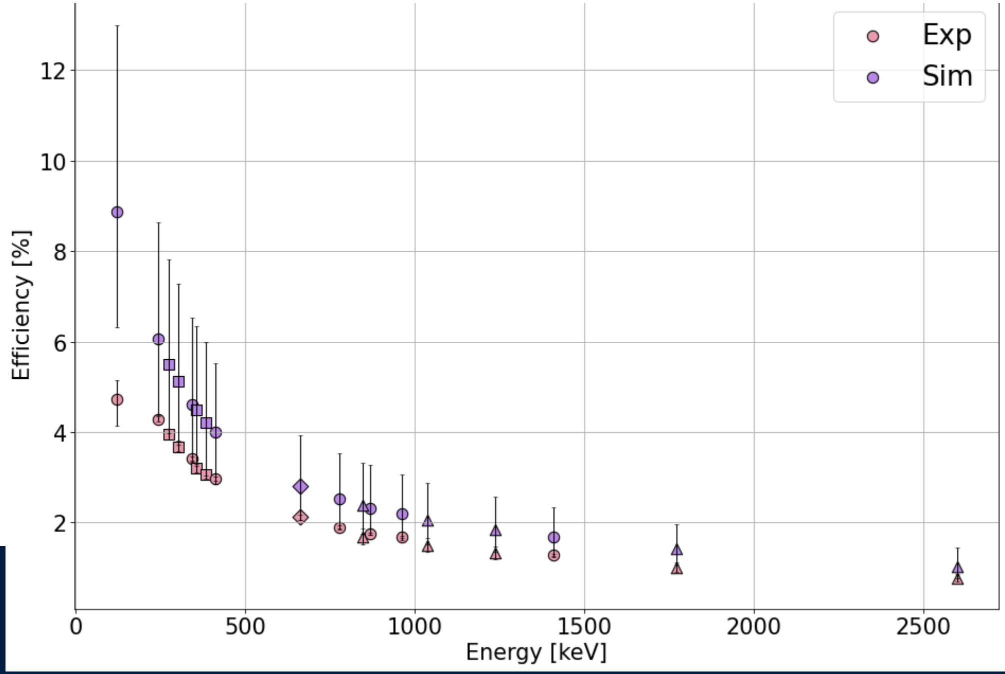

Impact of GEANT4 simulation

- Better optimization of the array in preparation for beam time
- Design of a better scintillator system for Bremsstrahlung mitigation (ongoing)
- Better understanding of the hypermet lineshape of the transitions (ongoing)
- Simulation of IDS in preparation for 2026 (ongoing)

ISOLDE Decay Station:
A large HPGe array with up to 15 clovers

IDS

- IDS is a permanent setup at CERN ISOLDE, used for the decay spectroscopy of exotic radionuclides.
- It consists of 12 HPGe clovers that can be placed in various configurations around a decay point equipped with a tape for activity build-up removal and charged particle detectors.
- Its support system is made of 5 gantries that can each host up to 3 clovers at once with various degrees of freedom for positioning.

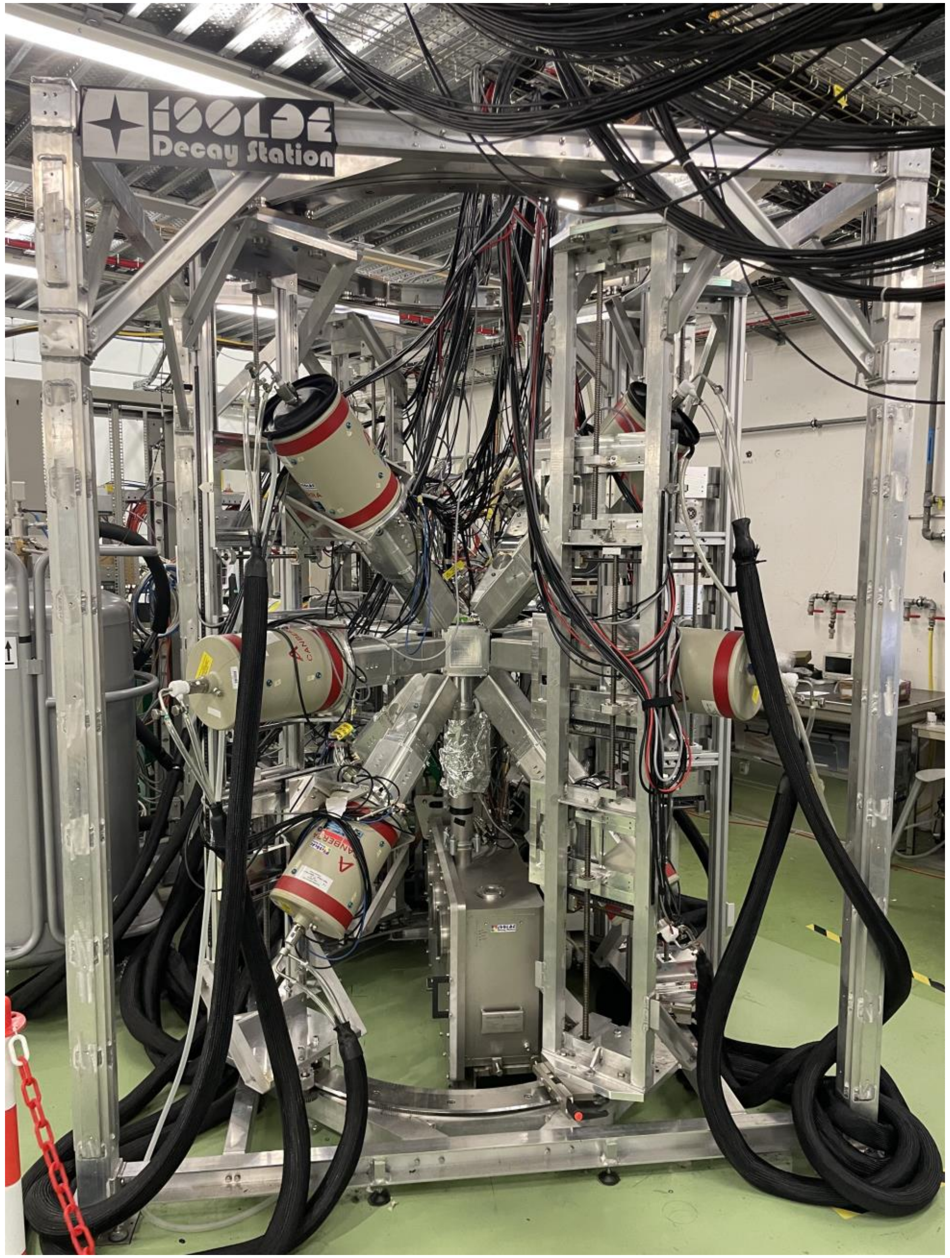

IDS Clover

2 new clovers received today at KU Leuven!!

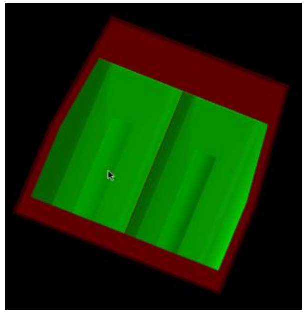

- Based on the Euroball design from Mirion with reduced distance from front to crystal.
- Each clover consists of 4 crystals with 23% relative size.
- With very thin layers between each crystal, it is possible to perform add-back to compensate for Compton scattering, resulting in an equivalent total size of 140% per clover.
- 2 of the clovers are equiped with a thin carbon windown to increase the dynamic range towards the lowest photon energies.
- A total of 15 clovers are available within the collaboration.

CERN LS3

- CERN is entering soon its next Long Shutdown.
- The ISOLDE facility will stop its activities from December 2025 until May 2028.
- During that period, IDS becomes available for measurements at other facilities.

➢ IDS is thus available to come to PSI for using its full potential in the 2026 muX and Reference Radii campaigns before the PSI long shutdown.

- The scope of that availability will be discussed at the next IDS Collaboration Meeting on 11-12 March 2025.

Back up:
Laser spectroscopy

Probing the nucleus through its electrons

Use lasers to scan for transition energies

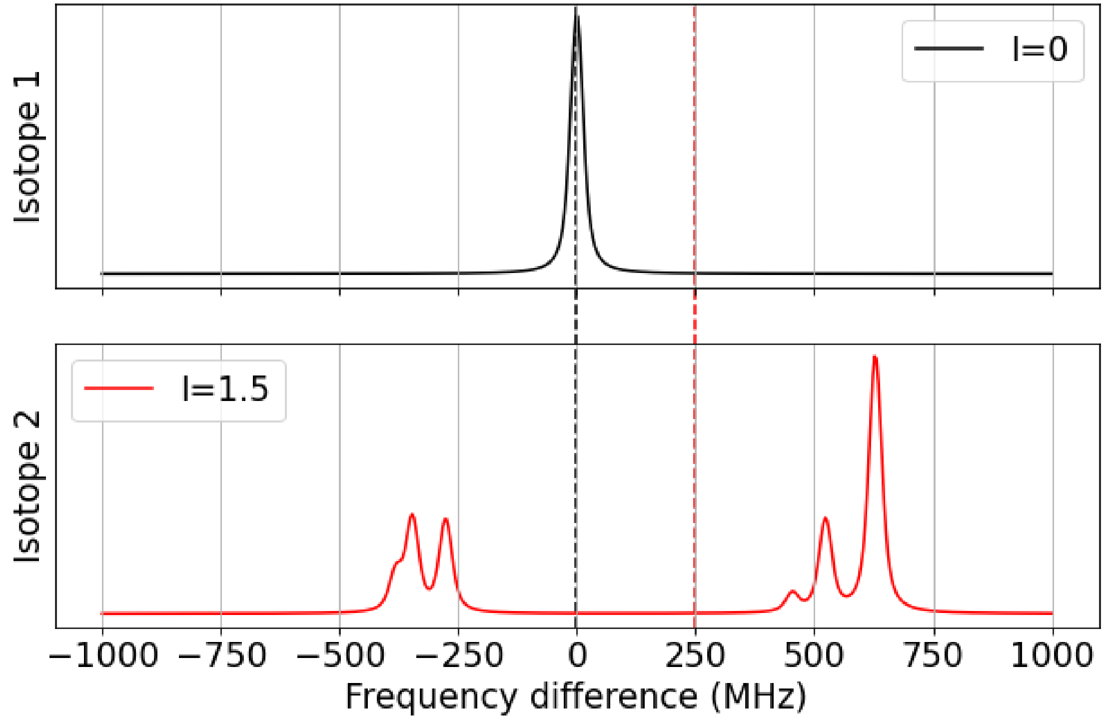

Introducing hyperfine splitting

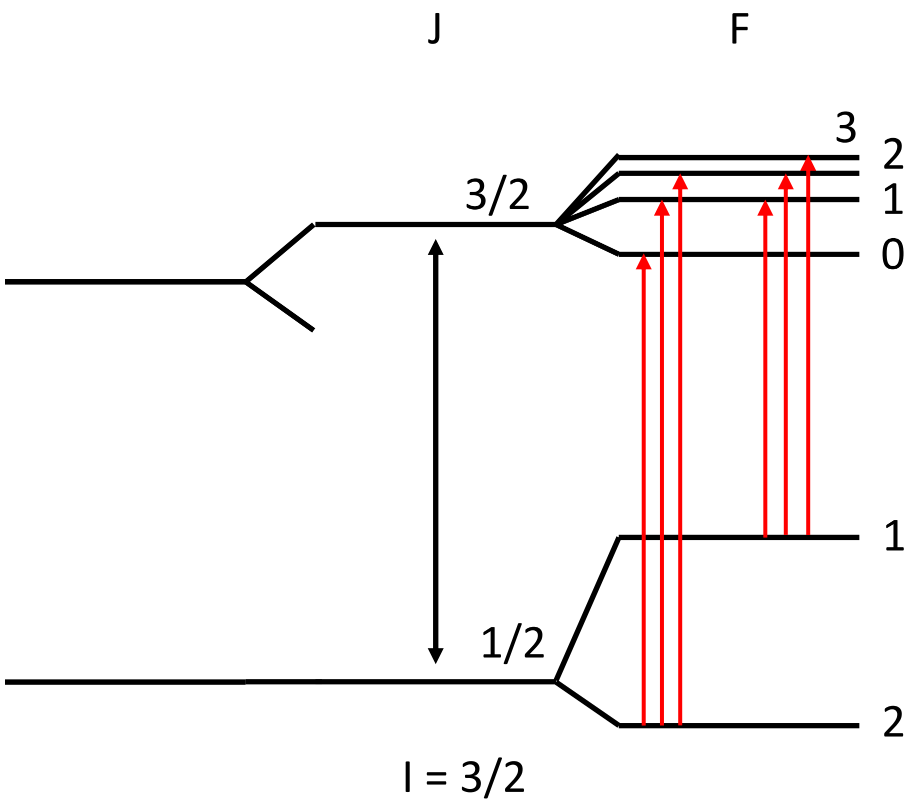

Probing the nucleus through its electrons

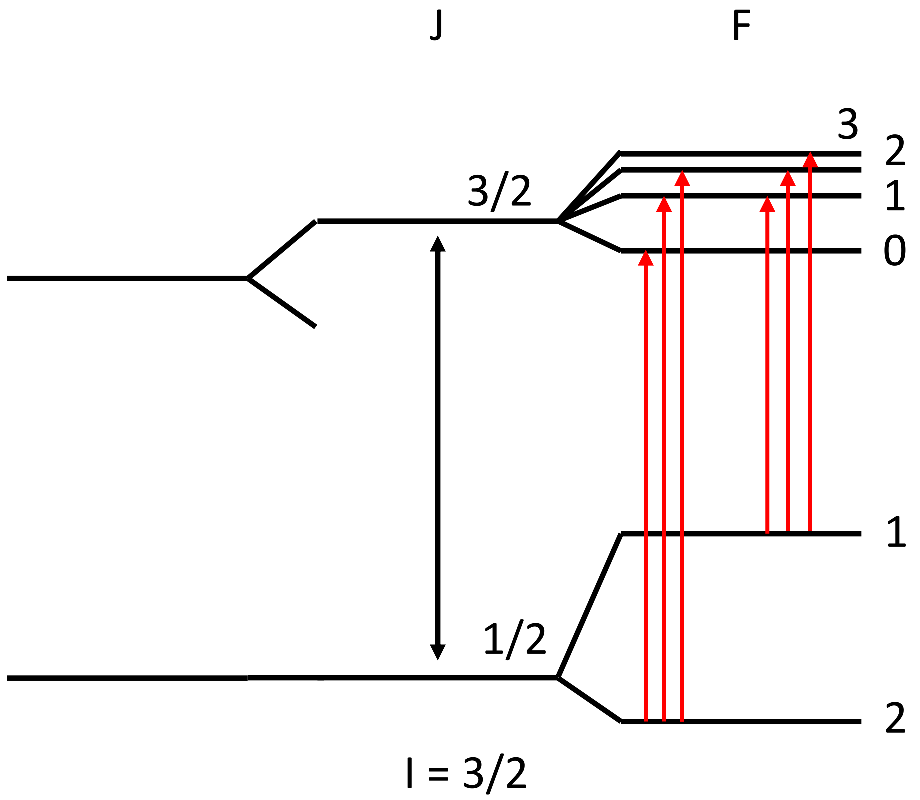

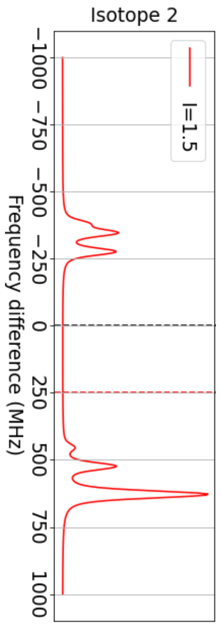

Fit for A_U, A_L, B_U, B_L

$$\Delta E_{HFS} = \frac{1}{2}\mathrm{AC} + \mathrm{B}\frac{\frac{3}{4}\mathrm{C}\,(\mathrm{C}+1) \;-\; \mathrm{I}(\mathrm{I}+1)\,\mathrm{J}\,(\mathrm{J}+1)}{2\mathrm{I}\,(2\mathrm{I}\;-1)\,\mathrm{J}\,(2\mathrm{J}\;-1)}$$

$$C = F\,(F+1) - I\,(I+1) - J\,(J+1)$$

$$A = \mu_I \frac{B_e(0)}{I\,J} \qquad \mathrm{B} = Q_s\, e\, V_{zz}(0)$$

Ratio between isotopes:
- Ratio of g-factors
- Ratio of quadrupole moments

KU LEUVEN